Return Differentials and the US Current Account

Patrick A. Hallan

October 1, 2025

Abstract

This paper studies the role of return differentials—the excess yield the United States earns on its external assets relative to what it pays on its liabilities—in shaping the U.S. current account. Using BEA international transactions and investment-position data, I construct quarterly measures of total, direct-investment (DI), and portfolio-investment (PI) return differentials for 2006Q1–2025Q1. Descriptive accounting shows that these wedges cumulate to trillions of dollars in effective current-account support, with DI persistently positive and PI more volatile. To identify causal effects, I estimate VARX models in levels and sign-restricted SVARs with DI, PI, monetary-policy, and exchange-rate shocks. The results show that DI shocks generate clear and persistent contractions in the current account balance, while PI shocks are smaller, less robustly signed, but quantitatively important for medium-horizon variance. Forecast-error variance decompositions indicate that return-differential shocks account for about one-tenth of CA/GDP fluctuations, comparable to monetary and exchange-rate shocks. Additionally, Historical decompositions link these dynamics to the global financial crisis, Covid-19, and phases of dollar strength. This paper interprets the evidence under the duality "exorbitant privilege-exorbitant duty" of the United States as the supplier of the key currency to the global economy.

1 Introduction

Return differentials—the excess yield the United States earns on its external assets relative to what it pays on its external liabilities—are a central but contested ingredient of U.S. external adjustment. They are invoked to explain why the United States has been able to run sizeable current-account (CA) deficits while still recording a persistently positive net primary-income balance and only gradual changes in its net international investment position (NIIP). In this paper, I ask a simple question: to what extent, and through which channels, do return differentials—especially those associated with direct investment (DI) and portfolio investment (PI)—move the U.S. current account?

The motivation is the well-known structural transformations post-1970s shift in the U.S. external balance sheet. Since the early 1980s the current account (CA) has often been negative and the net international investment position (NIIP) increasingly so, yet income from U.S. foreign assets has exceeded payments on foreign holdings of U.S. assets for most of the period. Two episodes sharpen this contrast: during the global financial crisis and again around Covid-19, swings in global risk and dollar conditions left quantity positions large and volatile, while the U.S. primary-income surplus proved resilient. This juxtaposition suggests that return differentials—excess yields on U.S. external assets relative to liabilities—are a key channel linking valuation and income flows to the external balance (Gourinchas and Rey, 2007).

Recently, the external environment facing the United States has changed in ways that make these return wedges even more salient. The post-zero-lower-bound normalization, the 2021–2022 inflation surge, and the repricing of term premia have pushed long-maturity U.S. interest rates higher, raising debt-service costs and testing perceptions of fiscal credibility. At the same time, a more contested global order raises questions about the durability of the U.S. "safety premium" and the dollar's ancillary advantages (see Rogoff, 2025). In this setting, quantifying how much—and through which channels across direct investment (DI) and portfolio investment (PI)—return differentials move the U.S. current account is not only an accounting exercise but a test of how external privileges interact with higher real rates and evolving global demand for U.S. assets.

This paper makes three contributions. First, on measurement and accounting, I assemble quarterly series (2006Q1–2025Q1) for DI and PI return differentials from BEA ITA/IIP data, and map these gaps into dollar flows via a transparent midpoint valuation, cumulating to show a multi-trillion-dollar contribution of return differentials to the U.S. CA over the sample. I pair this with a "Curcuru-inspired" [cite Curcuru] decomposition that separates the composition effect (what the U.S. holds and issues) from the return effect (how those positions are remunerated), and with descriptive evidence on the risk–safe mix of U.S. external positions. Second, on identification, I estimate VARX models in levels and sign-restricted SVARs that isolate DI- and PI-driven return-differential shocks. The results show that DI shocks deliver economically large and persistent improvements in the CA via net investment income, while PI shocks are not as directionally clear; these findings are robust to unit-root, lag-length, residual, break, Granger, and Toda–Yamamoto checks. Third, on interpretation, the evidence clarifies the channels behind the U.S. "exorbitant privilege": the DI margin dominates in levels and dynamics, whereas PI plays a thinner, risk-cycle-sensitive role.

The remainder of the paper proceeds as follows. Section 2 reviews the related literature, situating the debate on return differentials within the broader discussions of U.S. external privilege, global imbalances, and international financial hierarchy. Section 3 provides an overview of return differentials, including their measurement, empirical patterns, and decomposition into composition and return effects, with attention to the relative roles of direct and portfolio investment. Section 4 describes the data sources and construction of the quarterly series on return differentials and control variables. Section 5 outlines the econometric framework, including the VARX specification, identification strategy, and sign-restricted SVAR design. Section 6 presents the empirical results: baseline VARX responses, structural evidence from SR–SVARs, forecast-error variance decompositions, and historical decompositions. Section 7 concludes by synthesizing the contributions, discussing implications for the U.S. external position and global financial hierarchy, and suggesting avenues for further research.

2 Related Literature

The modern debate on U.S. external privilege sits at the intersection of international macroeconomics and international political economy. On one side, the "exorbitant privilege" view emphasizes that issuing the reserve currency confers structural advantages—deep, liquid markets; policy space; and the capacity to finance deficits at favorable terms—producing systematically higher returns on U.S. external assets than on its liabilities (Gourinchas and Rey, 2007). On the other, classic "key currency" (Williams, 1934)and hegemonic-stability (Waltz, 2018, Gilpin, 1971, Kindleberger, 1986) traditions stress that leadership entails obligations: supplying global liquidity, stabilizing markets in crises, and underwriting open-system public goods. In this framing, U.S. privilege coexists with "duties" that can be costly in stress episodes.

Return-differential (RD) debates are one leg of this broader dispute. In the early–mid 2000s, a quasi-consensus formed that the United States did enjoy a positive return wedge. The government's own assessment acknowledged it (ERP, 2003), and independent analyses echoed the point (e.g. Godley, 2003, Hung and Mascaro, 2004). The question gained salience as China's WTO accession and export surge widened U.S. trade deficits and compressed some traditional comparative advantages. RD therefore offered a compelling channel through which the United States could sustain external imbalance while cushioning net investment income.

By the mid-2000s, two positions crystallized. The "exorbitant privilege" camp (Gourinchas and Rey, 2007) documented persistent excess returns—especially linked to equity-like claims—and argued they materially support the U.S. external position via valuation and income effects. A challenger camp questioned either the measurement or the magnitude. Curcuru et al., 2008 showed that mixing revised positions with unrevised flows overstated portfolio gaps and, using consistent data and a breakdown of RD into composition (class weights) and return (with class) effects, found modest composition effects and limited within-class premia, with timing/trading effects doing more work. Also against the existence of systemic RD, Gros, 2006 argued the “black hole” is largely an accounting artifact that deflates true excess returns, while Hausmann and Sturzenegger, 2006 reframed the income surplus as “dark matter,” that is, unmeasured intangibles that, if capitalized, would turn the puzzle from abnormal returns into missing wealth.

In the 2010s, RD debates partly gave way to those on the macro challenges of the post-GFC environment, such as zero lower bound (L. Summers, 2013, L. H. Summers, 2016) and social, economic, and demographic structural changes (Gordon, 2017) leading to secular stagnation. Also contributing to place RD behind the scenes of academic and policy concerns, several U.S. external-balance margins improved: the maturing shale revolution, rising services surpluses, and a durable primary-income surplus partly offset a still-negative current account. In this context, RD remained relevant but less front-and-center than crisis management and the slow-growth policy debate.

Two developments nonetheless pushed the RD research agenda forward. First, Ali, 2016 used industry-level data to show that DI-linked excess returns may exceed what macro aggregates imply. Second, Gourinchas and Rey, 2022 synthesized privilege with “exorbitant duty,” embedding U.S. external returns and valuation into the global financial cycle: the U.S. is long risky and short safe, earning premia in tranquil times yet absorbing stress when global risk reprices.

Most recently, a global perspective has broadened the lens. Akyüz, 2021 highlights that many emerging economies face the mirror image—low-yielding assets and high-yielding liabilities. Mayer, 2021 and Nievas and Sodano, 2024 document the cross-country distribution of return differentials over long horizons. These studies show that RD is not solely a U.S. phenomenon but part of a broader hierarchy of international balance sheets, with significant incidence on developing and emerging economies and a recent shift from a uniquely U.S. privilege toward a wider “rich-world privilege.”

3 Return Differentials — An Overview

Return differentials (RD) are the yield gap between U.S. external assets and liabilities. Let r_t^A and r_t^L be the aggregate yields on assets and liabilities in period t, each measured as income over the lagged position (annualized for quarterly data):

$$r_t^A = \lambda \frac{I_t^A}{P_{t-1}^A}, \qquad r_t^L = \lambda \frac{I_t^L}{P_{t-1}^L},$$

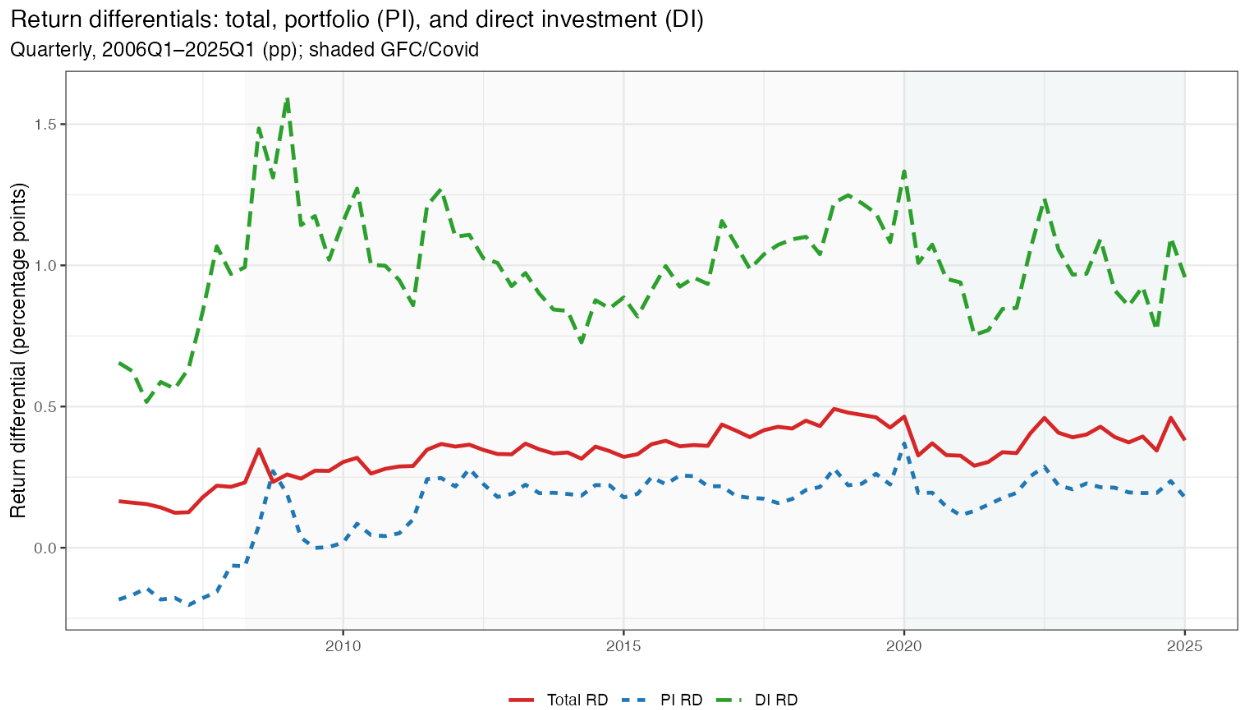

Figure 3.1: Return differentials: total, portfolio (PI), and direct investment (DI). Quarterly, 2006Q1–2025Q1 (percentage points). Shaded areas denote GFC (gray) and Covid (blue).

where I_t^A (I_t^L) is investment income on assets (liabilities), P_{t-1}^A (P_{t-1}^L) is the beginning-of-period stock of external assets (liabilities), and $\lambda = 4$ for quarterly data ($\lambda = 1$ for annual). The return differential is

$$RD_t = r_t^A - r_t^L.$$

Three facts stand out (see Figure 3.1). First, the DI return differential is persistently and substantially positive—roughly 0.8–1.2 pp through most of the sample—with a temporary post-GFC spike above $1\frac{1}{2}$ pp. Second, the PI return differential, while smaller than DI, rises meaningfully after the GFC: from near zero pre-2009 to systematically positive levels in the 2010s (about 0.1–0.3 pp), with clear cyclicality around risk episodes (compression in 2020 and rebound thereafter). Third, the total RD remains positive and trends up through the 2010s, dips during the Covid shock, and then recovers. These dynamics motivate identifying separate DI- and PI-driven RD shocks and lead us to expect stronger, more persistent current-account effects from DI innovations, with PI playing a thinner but growing role. [1]

I then estimate the cumulative dollar impact of RD on the US current account (Figure 3.2). To do so, I use a counterfactual argument that assumes both yield on asset and yield on liabilities to be equal (RD = 0). I assume a midpoint yield (the average between assets and liabilities) for total, DI, and PI, deflate each flow to 2015 USD using

[1] Appendix A.1 documents of the evolution of U.S. NIIP, DI, and PI balance sheets since 2006.

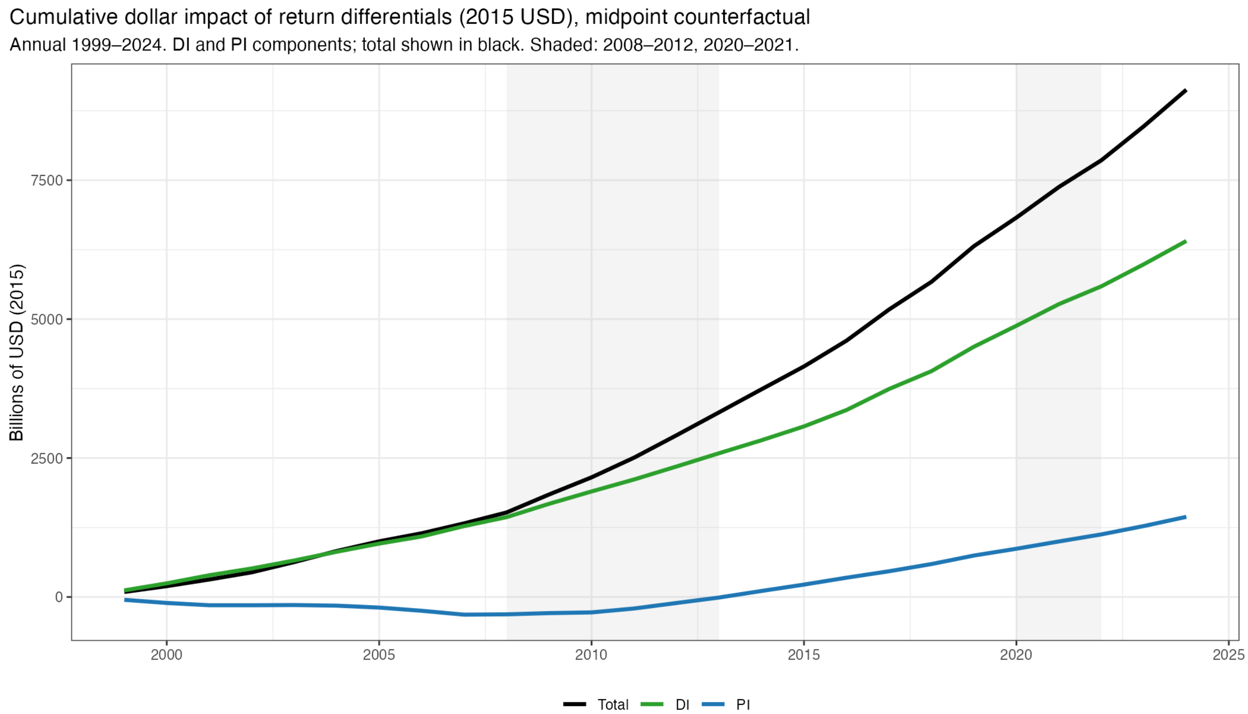

Figure 3.2: Cumulative dollar impact of return differentials on the U.S. current account, 1999–2024, in 2015 USD. Black = total; green = direct investment (DI); blue = portfolio investment (PI). Annual flows use the midpoint counterfactual $RD_t \times \frac{A_t+L_t}{2}$, deflated by CPI (2015=100) before cumulation. Shaded bands: 2008–2012 (GFC/Euro) and 2020–2021 (Covid).

CPI rebased to 2015=100, and calculate the difference from 1999 to 2024. This procedure converts yield gaps into the cumulative contribution of RD to net primary income—and hence to the current account—in real terms.

Figure 3.2 shows a large and steady build-up: the real cumulative impact exceeds roughly $9 trillion (2015 USD) by 2024. Compositionally, DI accounts for the bulk of the total by the end of the sample, while PI is modestly negative in the mid-2000s, turns positive after the GFC, and contributes an increasingly meaningful share through the 2010s–2020s. Shaded windows (2008–2012; 2020–2021) highlight that the upward drift persists despite crisis episodes, consistent with persistently higher returns on U.S. external assets—especially DI—relative to liabilities.

To understand how and to what extent each asset class impacts overall U.S. RD, I decompose the annual external yield differential into composition and return effects following the portfolio-accounting approach in Curcuru et al., 2010 and Curcuru et al., 2013. Let us break US holdings into five broad classes, direct investment (DI) equity, DI debt, portfolio investment (PI) equity, PI debt, other investment (OI). For each class (represented by $_c$), define asset and liability yields $r^A_{c,t}$ and $r^L_{c,t}$ as investment income over lagged positions (annualized), and portfolio shares $w^A_{c,t}$ and $w^L_{c,t}$ as the class's lagged position divided by the side's total (shares sum to one on each side). The aggregate differential

$$\Delta r_t = \sum_c w^A_{c,t} r^A_{c,t} - \sum_c w^L_{c,t} r^L_{c,t}$$

can be written as

$$\Delta r_t = \underbrace{\sum_c \big(w^A_{c,t} - w^L_{c,t}\big)\,\bar{r}_{c,t}}_{\text{Composition effect}} + \underbrace{\sum_c \bar{w}_{c,t}\,\big(r^A_{c,t} - r^L_{c,t}\big)}_{\text{Return effect}}, \quad \bar{r}_{c,t} \equiv \tfrac{1}{2}(r^A_{c,t} + r^L_{c,t}), \quad \bar{w}_{c,t} \equiv \tfrac{1}{2}(w^A_{c,t} + w^L_{c,t}).$$

With this, I can determine whether RD derives from the U.S. holding more of the high-yield categories (composition effect) or from higher earnings within each category (return effect). [2]

Figure 3.3 shows that at the whole portfolio level, the blue bars (return effect) account for nearly all of the positive yield differential over 1999–2024. The red bars (composition effect) are small on average and often negative before the GFC, turn mildly positive around 2009–2012, and remain close to zero thereafter. The black line (total) sits in the 1–2 pp range through most of the 2010s, dips around Covid, and then recovers. This indicates that the U.S. advantage is predominantly a within-category pricing phenomenon rather than the result of an especially high-yield portfolio mix.

Figure 3.4 stacks, for each class, the composition effect (difference in asset–liability weights evaluated at mid-returns, red) and the return effect (within-class yield gap evaluated at mid-weights, blue); the black line is the category's total contribution in percentage points. DI equity lifts the aggregate most. The return effect is large and persistent (1.0–1.3 pp most years) and even ticked up in the 2010s. By contrast, the composition effect was strongly positive pre-GFC (roughly 0.4–0.7 pp) but drifted down thereafter (closer to 0.2–0.4 pp by the early-2020s). This points to a gradual rise in the liability share of DI equity—diluting the U.S. "long-equity" tilt—partly offset by a resilient (and at times stronger) DI return advantage. The total stays high (black line 1.3–2.0 pp), dips around 2020, and recovers. DI debt sees a clear upward trend from negative to roughly neutral. The composition term is negative pre-2007 (–0.10 to –0.15 pp), reflecting a liability-heavy DI-debt mix, but trends toward zero after 2010 and is near-neutral by 2022–24. The return effect is small, slightly positive (a few basis points). Net, DI debt moves from a consistent negative contribution in the 2000s to "approximately zero" in recent years.

As for PI equity, over the period of analysis, the composition effect rises from 0.10–0.15 pp pre-GFC to 0.25–0.35 pp by the late-2010s, and the return effect climbs from 0.10 pp to 0.25–0.30 pp. The total contribution increases steadily (peaking around 0.6–0.7 pp), is briefly compressed in 2020, then re-establishes at a high level. This mirrors the secular deepening of outward and inward equity portfolios and a modest—but persistent—U.S. equity-return edge. Similar to DI debt, PI debt also sees a positive trend led by the composition effect. It is strongly negative in the early 2000s (–1.0 pp or worse), consistent with the U.S. issuing a lot of safe debt to the rest of the world; it improves materially over time, hovering around –0.3 to –0.5 pp by 2024. The return effect is small and only slightly positive. The total contribution stays negative throughout, but the drag shrinks meaningfully after 2010.

[2] All quantities are computed from BEA ITA/IIP income and positions; derivatives are excluded and reserves enter OI on the asset side as noted in the data appendix.

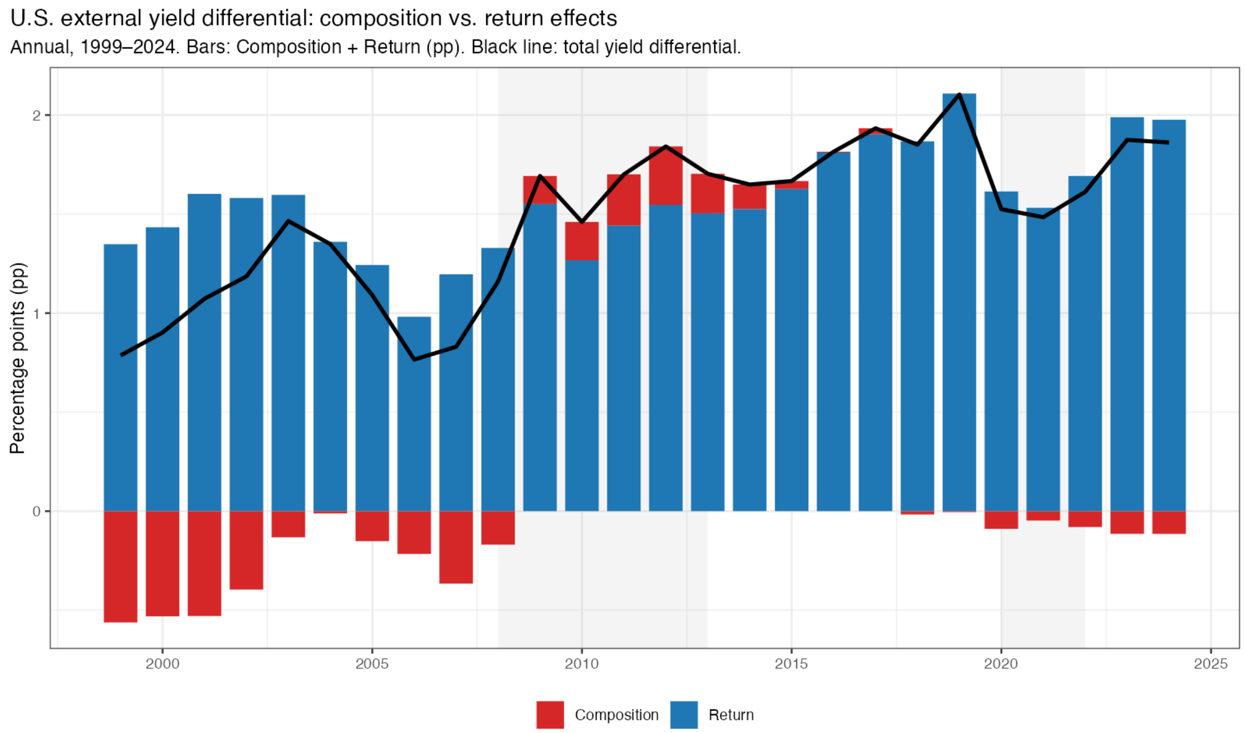

Figure 3.3: U.S. external yield differential: composition vs. return effects (annual, 1999–2024). Bars stack the composition (red) and return (blue) contributions in percentage points; the black line is the total yield differential. Shaded bands indicate 2008–2012 (GFC/Euro) and 2020–2021 (Covid).

Putting it together, two broad shifts line up with your observations: (i) in the debt classes (especially PI debt, but also DI debt) the composition effect moves from clearly negative in the 2000s toward less negative/slightly-positive in the 2010s; (ii) in equity classes, DI equity's composition advantage eases over time—partly offset by a stronger return effect—whereas PI equity sees both composition and return effects trend up. Summed at the aggregate, this is why the blue bars dominate in Figure 3.3: the U.S. advantage is primarily a within-category pricing/return phenomenon driven by equity (DI most of all), while the long-standing composition drag from debt has moderated but not disappeared.

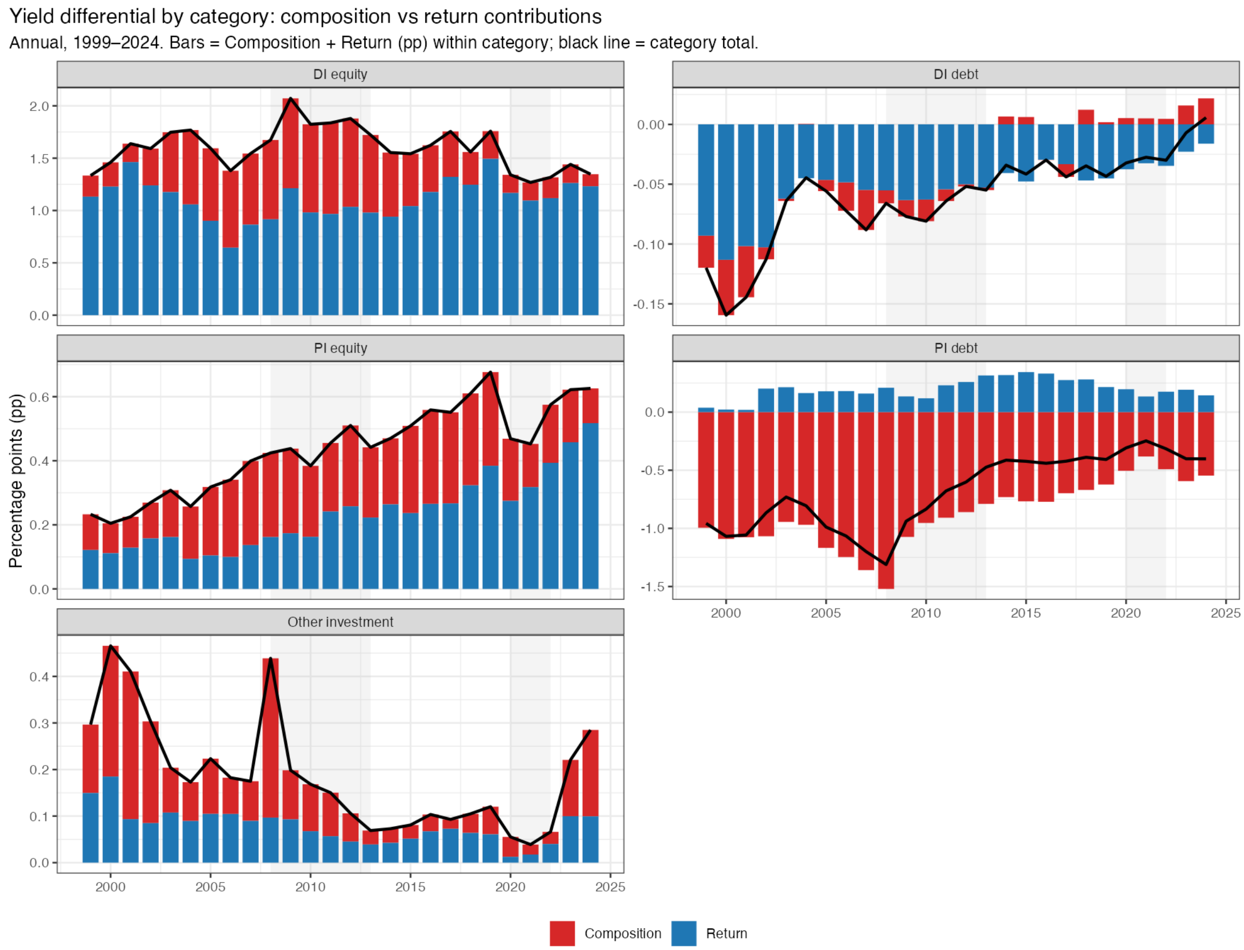

Figure 3.4: Yield differential by category: composition vs. return contributions (annual, 1999–2024). Panels show DI equity, DI debt, PI equity, PI debt, and other investment. In each panel, bars stack composition (red) and return (blue) in percentage points; the black line is the category's total contribution. Shaded bands indicate 2008–2012 (GFC/Euro) and 2020–2021 (Covid).

4 Data

The core dataset is quarterly, 2006Q1–2025Q1, and combines BEA International Transactions Accounts (ITA) and International Investment Position (IIP) with standard macro-financial controls. The dependent variable is the current account as a share of GDP (CA/GDP, `CAGDP`). Control variables are U.S. real GDP growth (g), rest-of-world growth (`g_star`), the broad real effective exchange rate (`REER`), the federal funds rate (`FFR`), the VIX (`VIX`), and two crisis dummies (`GFC`, `Covid`). Exact series definitions for `g_star` and `REER` are documented in the Appendix.

Return differentials. Category yields are defined as income divided by the beginning-of-period (lagged) position (annualized where needed), and the aggregate return differential as the asset-weighted average yield minus the liability-weighted average yield:

$$r_t^{\text{diff}} \equiv r_t^A - r_t^L, \qquad r_t^A = \frac{\text{Income on assets}_t}{\text{Assets}_{t-1}}, \quad r_t^L = \frac{\text{Income on liabilities}_t}{\text{Liabilities}_{t-1}}.$$

I report a total differential (`r_diff`) and differentials for direct investment (DI; `r_diff_DI`) and portfolio investment (PI; `r_diff_PI`). Returns are stored as fractions in the code and multiplied by 100 when presented (`r_diff_pp`, etc.).

`GFC` and `Covid` are quarterly dummies included as exogenous controls and represent the two major shocks in the Global economy. Exact date ranges are listed in the Appendix.

I parse quarters from the raw spreadsheets, restrict to 2006Q1–2025Q1, coerce numeric types, and keep return measures in percentages only for presentation. For VARX, I build per-specification endogenous blocks

$$Y_t = \big(\texttt{CAGDP}, \texttt{g}, \texttt{g\_star}, \texttt{REER}, \texttt{FFR}, r^{\text{diff}}\big)_t,$$

with $r^{\text{diff}} \in \{\text{total}, \text{DI}, \text{PI}\}$, and a common exogenous block $X_t = (\texttt{VIX}, \texttt{GFC}, \texttt{Covid})_t$, both at quarterly frequency. Variables entering the VAR are unit-free ratios, growth rates, or interest-rate levels. In descriptive accounting figures (e.g., cumulative dollar impacts), I convert IIP positions from millions to billions of USD to match GDP units and apply the midpoint valuation $r_t^{\text{diff}} \times \frac{A_t + L_t}{2}$. These unit conversions affect only the descriptive exercises, not the econometrics.

5 Methods

5.1 Identification

I study how return-differential shocks move the U.S. current account. The design of the VARX model is

$$\mathbf{y}_t = \begin{bmatrix} \text{CAGDP}_t \\ g_t \\ g_t^* \\ \text{REER}_t \\ \text{FFR}_t \\ r_t \end{bmatrix}, \qquad \mathbf{x}_t = \begin{bmatrix} \text{VIX}_t \\ \text{GFC}_t \\ \text{Covid}_t \end{bmatrix},$$

where $\mathbf{y}_t$ is the endogenous block and $\mathbf{x}_t$ the exogenous block. CAGDP is the current account (share of GDP), g and g^* are U.S. and rest-of-world real growth, REER is the real effective exchange rate (higher = real appreciation of the dollar), FFR is the policy rate, and r is the (total) external return differential in percentage points.[3] The exogenous block includes the VIX and two crisis indicators.

Pre-estimation diagnostics follow a standard sequence and motivate all modeling choices. First, unit-root tests (ADF, PP, KPSS) indicate near-integration in several series (CAGDP, REER, FFR, and the return differential) and stationarity in foreign growth, so the VAR with exogenous controls is estimated in levels to preserve long-run comovements while relying on bootstrap inference for impulse responses. Second, lag length is chosen by information criteria with a pragmatic baseline of $p = 2$ (balancing AIC/HQ/FPE vs. SC/BIC), and this choice is validated ex post by stability checks (all companion-matrix roots strictly inside the unit circle). Third, residual autocorrelation is assessed with Breusch–Godfrey LM and Portmanteau tests, which the system passes at conventional horizons; robustness to nearby lags is reported. Fourth, residual normality and ARCH–LM tests reveal non-Gaussianity and conditional heteroskedasticity concentrated in the growth and current-account blocks, reinforcing the use of bootstrap inference. Fifth, structural-stability diagnostics (Quandt–Andrews and Bai–Perron) point to breaks mainly around global-shock windows in the growth block, consistent with the inclusion of GFC and Covid dummies. Finally, Granger-causality checks confirm that return differentials have predictive content for the current account. The complete diagnostics are presented in Section 6.2.

Our baseline reduced-form model is thus a *VARX in levels with lag order* $p = 2$:

$$\mathbf{y}_t = \mathbf{c} + A_1\mathbf{y}_{t-1} + A_2\mathbf{y}_{t-2} + B\mathbf{x}_t + \mathbf{u}_t, \qquad \mathbf{u}_t \sim (\mathbf{0}, \Sigma_u). \tag{5.1}$$

I report generalized (Pesaran–Shin) impulse responses and forecast-error variance decompositions from the VARX in levels, computed with bootstrap confidence bands and invariant to variable ordering. For transparency, I scale shocks so that the impulse in r_{diff} (and, where appropriate, FFR and REER) corresponds to a one–percentage-point increase on impact; ordering-robust Cholesky responses are provided in the appendix. Structural interpretation is reserved for the sign-restricted SVAR reported below.

To move from reduced-form to structural interpretation, I estimate sign-restricted SVARs that discipline the contemporaneous interactions among return differentials, monetary policy, and the exchange rate. Recursive orderings are ill-suited given likely correlations across these shocks; sign restrictions impose only minimal structure—directional responses consistent with theory—while leaving dynamics to be data-driven. Three variants are considered: (i) a DI model, identifying shocks to the direct-investment return differential; (ii) a PI model, isolating portfolio-investment shocks; and (iii) a joint model including DI, PI, monetary, and REER shocks, which serves as the baseline. Structural shocks are scaled to a +1 pp move in their own variable, with inference based on identification bands. For each model, I report impulse-response functions, forecast-error variance decompositions, and historical decompositions

[3] Section 4 details construction; r is income over lagged positions.

to quantify the contribution of return-differential shocks to U.S. current-account fluctuations.

6 Results

6.1 Roadmap and econometric preliminaries

I estimate a quarterly VAR with exogenous controls (VARX) in levels on 2006Q1–2025Q1 U.S. data. The endogenous block is (CAGDP, g^*, g, FFR, REER, r_{diff}); exogenous controls are (VIX, GFC, Covid).

Shock normalization (drop-in). Throughout the paper, each identified shock is rescaled so that the impact response of its own variable equals +1 unit. Formally, if Θ_h denotes the (orthogonalized or sign-restricted) impulse-response matrices and i_j indexes the "own" variable of shock j, I report

$$\widetilde{\Theta}_h(:,j) = \frac{\Theta_h(:,j)}{\Theta_0(i_j,j)} \qquad (h=0,1,\ldots),$$

so that $\widetilde{\Theta}_0(i_j,j) = 1$. For return and rate variables—r_{diff}, $r_{\text{diff,DI}}$, $r_{\text{diff,PI}}$, and FFR—"+1 unit" corresponds to a +1 percentage point move on impact. For REER, "+1 unit" means a +1% appreciation when REER is in logs (or +1 index point when it is in levels). This is a scale convention only: forecast-error variance decompositions are invariant to it, while the magnitudes of other variables' IRFs scale accordingly. Inference uses (i) bootstrap confidence bands for reduced-form IRFs and (ii) identification bands for sign-restricted SVARs. Unit-root behavior in several variables, stability of the estimated VARX, and non-Gaussian/heteroskedastic residuals (notably in g, g^*, and CAGDP) motivate the levels specification with bootstrap inference. Full diagnostics and lag choice (p=2) are in Appendix B.

6.2 Diagnostics

Unit Root Tests The unit-root evidence in able B.3 follows a familiar macro pattern. For CAGDP, REER, the federal funds rate (FFR), and the total return differential r_{diff}, ADF, and PP tests fail to reject a unit root in levels but reject strongly after first differencing, while KPSS rejects level (and, where tested, trend) stationarity. The above variables are thus I(1). Foreign growth g^* is stationary across all tests (I(0)). U.S. growth g is borderline—mixed ADF/PP outcomes in levels with KPSS not rejecting stationarity—so I treat g as I(0) and verify robustness using differences. This mixture of near-integrated ratios/rates and stationary growth rates motivates estimating the VAR with exogenous controls in levels, which preserves potential long-run comovements that differencing would remove and is consistent for impulse responses in large samples.

Lag-Length Tests To decide on the lag dimension of the VARX model, I proceed with standard lag-length tests. Table B.1 shows that AIC, HQ, and FPE select the maximal lag ($\hat{p} = 8$) in our search window, while SC/BIC selects a parsimonious model ($\hat{p} = 1$). Because AIC/HQ penalize complexity more weakly than SC, they often drift upward in small-to-moderate samples when dynamics are rich. Given our sample size (quarterly 2006Q1–2025Q1) and six endogenous variables plus exogenous controls, I adopt $p = 2$ as a compromise: it is much less parameter-intensive than $p = 8$ yet captures the short-run dynamics that $p = 1$ misses.

VAR Stability/Root of Characteristic Polinomial Table B.4 shows that both the $p = 1$ and $p = 2$ specifications are dynamically stable: all companion–matrix eigenvalues lie strictly inside the unit circle (no moduli ≥ 1). The baseline $p = 2$ model provides a slightly larger cushion from the unit–root boundary (largest modulus ≈ 0.951 versus ≈ 0.984 for $p = 1$), implying shocks are persistent but mean–reverting. This validates the use of orthogonalized IRFs and FEVDs from the levels VAR and supports our choice of $p = 2$ as the primary specification, while retaining $p = 1$ as a useful robustness check.

Residual autocorrelation Table B.5 shows Breusch–Godfrey LM tests run equation by equation. The g and g^* equations reject the null of no serial correlation across all horizons (h=4, 8, 12, $p < 0.01$), while the CAGDP, REER, FFR, and r_{diff} equations do not exhibit significant autocorrelation at conventional levels. Panel B aggregates system–wide diagnostics. At moderate horizons the system Portmanteau tests can be tight (e.g., adjusted $Q(8)$, p=0.045), but at h=12 both the Breusch–Godfrey LM (p=0.265) and the asymptotic Portmanteau (p=0.542) fail to reject serial independence, indicating that the VARX(p=2) passes the global serial correlation checks at the longest commonly used horizon. Taken together, these results suggest that while some autocorrelation persists in the GDP growth blocks (g, g^*), the overall system is adequately whitened for inference; as a robustness step, I will (i) report IRFs with bootstrap bands (already implemented) and (ii) probe p=3–4 in an appendix to verify that our main results for CAGDP are not sensitive to additional lags.

Residual normality and heteroskedasticity of VARX innovations Residual diagnostics (summarized in Appendix **??**) reveal that some equations (returns, interest rate, and REER) produce innovations that are close to Gaussian, while growth and current account residuals exhibit clear departures due to fat tails and skewness. This pattern is common in macro VARs: shocks to real activity and external balances are crisis-prone and non-Gaussian. To account for this, all inference in this paper relies on bootstrap methods, which remain valid under such departures from normality.

In addition to non-normality, residuals were also tested for heteroskedasticity using ARCH–LM procedures. Results, reported in Appendix **??**, show that the same variables identified as non-Gaussian—namely g, g^*, and CAGDP—also exhibit conditional heteroskedasticity, while FFR, REER, and the return differential do not. This reinforces the interpretation that volatility clustering and fat-tailed shocks are intrinsic features of the growth and external balance series in this system. The joint diagnostics further justify the use of bootstrap inference in the VARX analysis, ensuring that confidence intervals properly reflect the non-normal, time-varying nature of the innovations.

STRUCTURAL STABILITY I assess structural stability of the VARX($p = 2$) system using the Quandt–Andrews family of coefficient tests (supF, aveF, expF) and Bai–Perron tests for breaks in residual variance. The results are reported in Table B.9. For the return differential (r_diff^{pp}), the average F-test rejects stability at the 5% level whereas the supF statistic is only marginally significant (10%), indicating moderate but diffuse coefficient drift rather than a single sharp break. Foreign growth (g^*) displays decisive instability: all three coefficient tests strongly reject ($p < 0.001$) and two variance breaks are identified at 2019Q3 and 2022Q2, spanning the COVID shock and its aftermath. Domestic growth (g) also rejects coefficient stability at conventional levels, although no variance break is detected. By contrast, the federal funds rate (FFR) and the real effective exchange rate (REER) show no evidence of variance breaks and do not exhibit sharp coefficient instability. Finally, CAGDP features one variance break around 2021Q4 but no sharp coefficient instability. Taken together, instability concentrates in the growth block (external and domestic) and, to a lesser extent, in CAGDP's volatility. This pattern aligns with the residual diagnostics: periods of elevated global and domestic macro uncertainty manifest as both non-Gaussian innovations and time-varying volatility in the growth channels. Inference based on bootstrap impulse responses is therefore warranted and adopted in subsequent sections.

GRANGER CAUSALITY INTO CAGDP Table B.10 summarizes Granger causality tests that assess whether return differentials help predict fluctuations in the U.S. current account balance. Across specifications, the null hypothesis that return differentials have no predictive content for the current account is strongly rejected. In the baseline Granger test, lagged return differentials (r_diff_pp) significantly improve forecasts of the current account, with p-values below the 1% level.

The results are robust to two important extensions. First, the block exogeneity test shows that return differentials, the real effective exchange rate (REER), and the federal funds rate (FFR) jointly Granger-cause the current account, confirming the relevance of macro-financial conditions alongside relative returns. Second, the Toda–Yamamoto procedure, which guards against potential non-stationarity by augmenting the lag length, produces nearly identical conclusions. Taken together, these results underscore the central role of return differentials in shaping the U.S. external position, consistent with the argument that financial asymmetries allow the United States to sustain current account deficits without destabilizing reversals.

6.3 Baseline VARX

Having validated the VARX specification, I now turn to the impulse-response analysis. I begin with shocks to the total return differential before moving to disaggregated DI and PI shocks. Figure C.1 reports generalized impulse responses of the U.S. current account to shocks in the return differential, the policy rate, and the real exchange rate. A positive return-differential shock (+1pp) initially improves the current account but the effect is short-lived and reverses after a few quarters, suggesting that the adjustment operates through valuation and income channels that fade as liabilities reprice. By contrast, monetary and exchange-rate shocks display more cyclical profiles: a tighter FFR or a dollar appreciation both weigh on the current account, consistent with standard expenditure-switching and interest-rate parity channels. In all cases, bootstrap bands underscore the high volatility of external-balance dynamics at business-cycle horizons.

Figure C.2 examines the drivers of return differentials themselves. Foreign and domestic growth innovations exert positive but short-lived effects, while FFR and REER shocks transmit more persistently, lowering excess returns on U.S. assets relative to liabilities. These patterns align with the interpretation that return differentials capture the premium the U.S. earns when global growth is strong and financial conditions loose, but that advantage erodes when monetary tightening or dollar strength compresses yields. Together, the two panels confirm that the return differential is both a driver and a margin of adjustment: it directly affects the current account yet is itself shaped by macro-financial shocks.

6.4 Sign-Restricted SVAR

I move from the reduced-form VARX to structural interpretation using sign-restricted SVARs, since recursive orderings are implausible given contemporaneous co-movement among return differentials, monetary policy, and the real exchange rate; sign restrictions impose minimal directional structure while leaving magnitudes data-driven. Our main structural model is the Joint specification including DI- and PI-return-differential shocks alongside monetary policy (FFR) and the real exchange rate (REER). For robustness and disaggregation, I also estimate DI-only and PI-only variants.

Figure 6.1 reports the JOINT SR–SVAR impulse responses of CA/GDP to shocks in direct–investment (DI) and portfolio–investment (PI) return differentials, monetary policy (MP), and the real effective exchange rate (REER). For DI, the median response of CA/GDP is clearly negative on impact and remains below zero over several horizons before gradually mean–reverting. Although the 90% identification bands cross zero—reflecting that some admissible rotations imply weaker or even opposite responses—the posterior sign shares (Appendix Fig. D.1) are consistently above 50%, and often closer to 60–75%. This indicates that the bulk of admissible models support a negative DI effect, even if the direction is not pinned down in every rotation. By contrast, the PI shock produces a near–zero

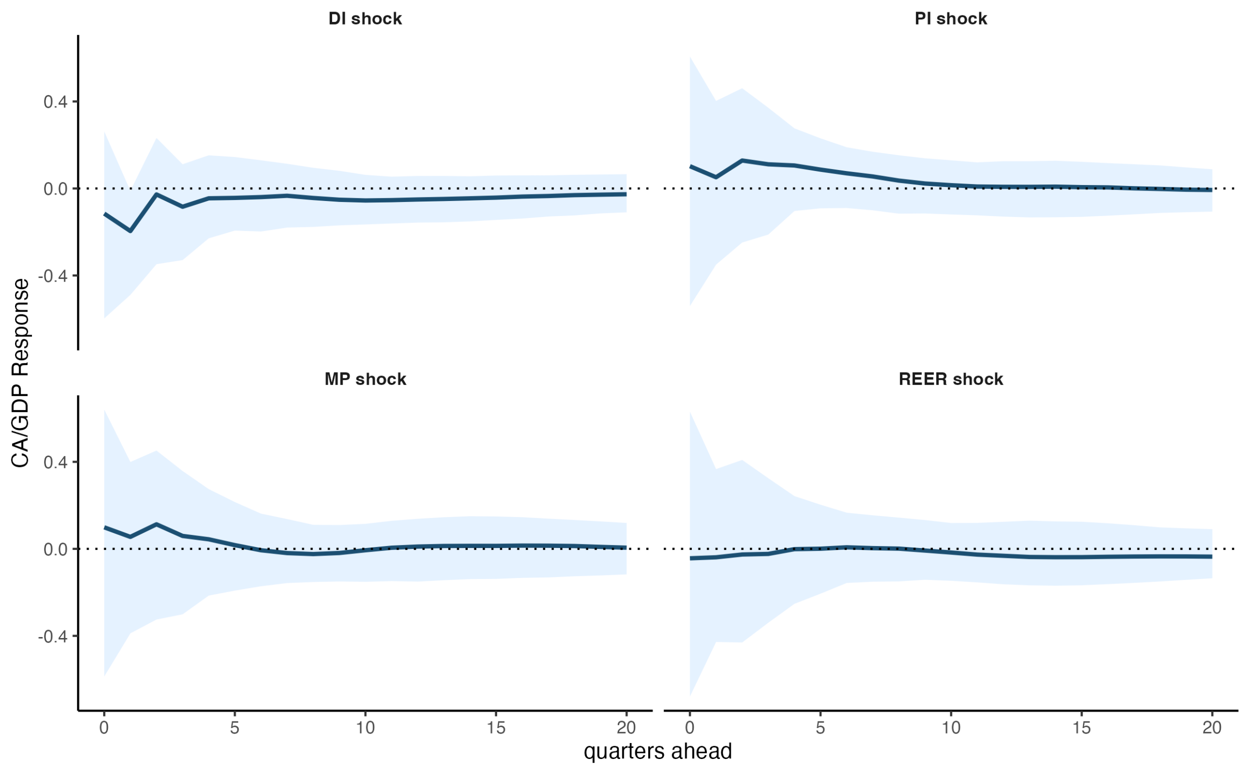

Figure 6.1: JOINT sign-restricted SVAR: impulse responses of CA/GDP to DI, PI, MP, and REER shocks (median with 90% bands).

median response in the short run and drifts only mildly negative at medium horizons, with sign shares hovering around 50%.

Table 6.1 and Fig. 6.2 summarize the FEVDs from the JOINT SR–SVAR. At horizons of one to five years, portfolio return-differential shocks account for roughly 9–10% of the variance in CA/GDP, slightly larger than the contribution of direct-investment shocks (around 6–7%). Monetary policy and REER shocks each contribute in a similar range (9–11%). These shares are medians across admissible rotations; bands are wide, reflecting identification uncertainty, but the relative ordering is consistent across horizons.

The impulse responses and FEVDs provide complementary views. DI shocks generate persistent and directionally negative movements in CA/GDP, with sign shares well above 50% across horizons, making them the cleaner and more robust channel. PI shocks, by contrast, produce weaker and less reliably signed responses, staying near zero in the short run and drifting only mildly negative in the medium run. Yet in the FEVDs, PI shocks account for a larger share of CA/GDP variance (around 9–10% versus 6–7% for DI). This pattern reflects the fact that FEVDs measure the contribution of shocks to forecast error variance across all admissible rotations, and medians of variance shares do not coincide with squared median IRFs. In short, DI provides stronger directional evidence; PI, despite weaker IRFs, absorbs a larger share of forecast variance in the joint system(Appendix D).

The monetary policy (FFR) and exchange-rate (REER) shocks provide useful benchmarks. The MP shock yields a

Table 6.1: FEVD of CA/GDP in the Joint SR–SVAR (median shares, %)

Horizon	DI	PI	MP	REER
4q	5.8	8.6	9.1	9.0
8q	6.5	9.4	9.6	9.6
12q	7.0	9.3	9.6	9.8
20q	6.9	8.9	9.5	9.8

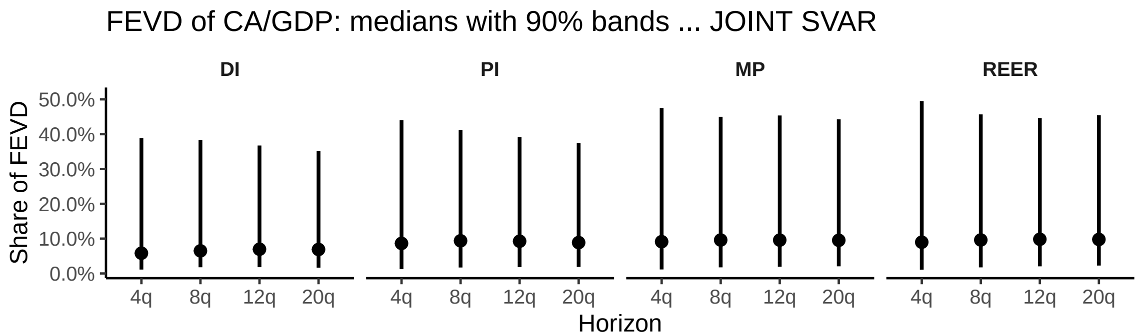

Figure 6.2: Forecast error variance of CA/GDP in the Joint SR–SVAR: median shares with 90% bands by horizon for DI, PI, MP, and REER shocks.

modest dip in CA/GDP that is short-lived in the IRFs, with sign shares hovering near 50% and wide identification bands. This indicates that while monetary tightening may put temporary pressure on the external balance, the direction and persistence of the effect are not strongly identified. By contrast, the REER shock—defined as a real appreciation—produces a small but more persistent negative effect on CA/GDP in the IRFs, with sign shares exceeding 50% at medium horizons. In the FEVDs, both MP and REER shocks account for around 9–11% of the variance in CA/GDP, comparable to the PI share and somewhat larger than DI. Thus, while DI shocks provide the clearest directional evidence and PI the largest variance share, MP and REER shocks remain material contributors to U.S. external-balance fluctuations, consistent with the broader adjustment mechanisms emphasized in the literature.

6.5 Historical Decomposition

Figure 6.3 presents the stacked historical decomposition of CA/GDP innovations under a representative admissible rotation of the main structural model (the Joint SR–SVAR). Each quarter's deviation is decomposed into the contributions of DI, PI, MP, and REER shocks. This visualization highlights how the combined impact of shocks explains most short-run fluctuations in the external balance. DI and PI shocks together account for large swings, while MP and REER shocks also feature prominently during specific episodes.

The stacked contributions reflect the interaction of impulse-response signs with the realized structural shocks. Because a positive DI shock worsens CA/GDP, a negative DI shock (risk-off) appears as a positive contribution

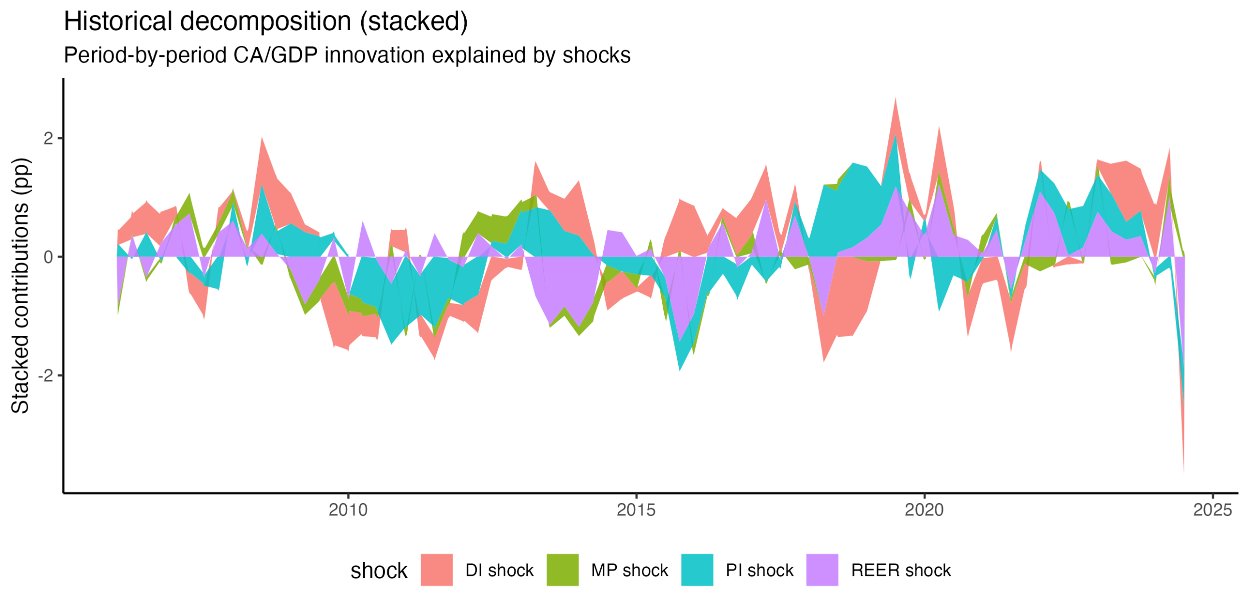

Figure 6.3: Historical decomposition of CA/GDP innovations (Joint SR–SVAR, representative admissible rotation). Notes: Period-by-period innovations are decomposed into the contributions of DI, PI, MP, and REER shocks. Positive areas reflect quarters in which the shock contributed to a higher CA/GDP balance; negative areas indicate the opposite. The stacked areas sum to the total CA/GDP innovation attributable to the identified shocks.

in the decomposition. PI shocks, whose IRFs are less directionally robust, also contribute substantially, but with alternating signs across episodes, reflecting the weaker directional identification discussed earlier. MP and REER shocks appear as secondary but still material drivers of short-run volatility.

The decomposition aligns closely with major global events: sharp DI and PI contributions around the Global Financial Crisis and COVID, REER-driven fluctuations during phases of sustained dollar strength, and MP shocks visible around episodes of U.S. monetary easing and tightening. Taken together, the HD underscores that return-differential shocks (both DI and PI) are key proximate drivers of U.S. external-balance fluctuations, even if their average direction is harder to pin down in the baseline SR–SVAR.

6.6 Interpreting the Role of Return Differentials

The structural evidence presented above clarifies both the scope and the limits of return-differential shocks in shaping the U.S. current account. Three points stand out. First, the analysis distinguishes the roles of direct- and portfolio-investment margins. DI shocks display clearer directionality in the impulse responses—persistently depressing CA/GDP on impact and over subsequent horizons—and their sign robustness is high across admissible rotations. Yet their variance share in the FEVD is comparatively modest (about 6–7%). PI shocks, by contrast, are weakly identified in direction but consistently explain a somewhat larger portion of medium-horizon volatility (roughly 9%), underscoring their quantitative relevance even if their sign is fragile. In other words, DI emerges as the structurally more reliable component of the U.S. return-differential advantage, while PI represents a more volatile and episodic channel whose effects are harder to pin down directionally but non-trivial in magnitude.

Second, the joint model highlights the interaction of return-differential shocks with policy and exchange-rate channels. Monetary-policy shocks contribute a variance share on par with PI, and REER shocks account for a comparable fraction of external-balance volatility. The historical decomposition shows that these forces interact non-trivially: episodes such as the GFC, the Covid shock, and phases of dollar strength feature concurrent (and sometimes offsetting) contributions from DI, PI, MP, and REER shocks. The results therefore position return differentials not as isolated curiosities but as integrated components of the broader macro-financial adjustment process.

Third, combining IRFs, FEVDs, and HD establishes a coherent narrative. IRFs capture the shape and timing of adjustment; FEVDs measure the relative importance of each channel; and the HD traces their realized contributions over crises and recoveries. The synthesis is that return differentials are neither a dominant nor a negligible force. Instead, they are material, medium-sized drivers whose effects rival those of monetary and exchange-rate shocks. Their influence is particularly salient in turbulent periods, when valuation effects amplify swings in the current account despite stable or improving net income balances.

Overall, the contributions of this section are twofold: empirically, it documents robust evidence that return-differential shocks explain a non-trivial share of U.S. external-balance fluctuations; conceptually, it refines the understanding of the “exorbitant privilege” by showing that DI anchors the privilege while PI produces greater variance pressures.

7 Conclusion

The analysis in this paper revisits the role of U.S. return differentials by addressing its impact on current account shifts. Since the structural shifts of the 1970s, the U.S. external position has been consistently deteriorating. More recently, with trade and financial liberalizations this deterioration has deepened, especially with China rising to the position of "factory to world commodities." In the 2010s, this trend is partly offset by three forces: the shale oil revolution positive impact on the trade balance, the deepening of the surplus position of the service account, and the improvement of the primary income account. This paper studied the key channels preventing the deterioration of the improvement of the US primary income account; DI and PI return differentials.

The paper makes three contributions. First, on the descriptive side, it documents new quarterly evidence on total, direct-investment, and portfolio-investment return differentials for 2006Q1–2025Q1, highlighting their distinct impacts; DI has a clearer directional role, while PI shocks produce greater variance. Second, using a VARX baseline and sign-restricted SVARs, it shows that return-differential shocks are non-trivial drivers of U.S. external-balance fluctuations, explaining a variance share comparable to monetary-policy and exchange-rate shocks. Within this, direct-investment shocks display clearer directional effects, while portfolio-investment shocks are weaker in sign but quantitatively more persistent. Third, the historical decomposition links these dynamics to global episodes—GFC, Covid, and dollar-cycle phases—demonstrating how return differentials interact with monetary and exchange-rate channels in shaping the current account.

Return differentials continues to be a key theme in international economics. While RD has been a support preventing deeper deficit of the US external position, it has clear limits. Quantitatively, the average of 0.8-1.2 pp of can only prevent the US primary income from entering negative territory to a limited extent as chronic trade deficit cumulatively worsens the external position. But probably more important are the recent shifts in the global economy such as the questioning of the role of US dollar as the reserve currency and the Fed's capacity to set the monetary policy independent from political pressure. In part, this was reflected in the event of the decoupling between uncertainty shock of the tariff hike and treasury yields. It has also been shown in the depreciation of the US dollar vis-à-vis other central currencies and, more importantly, against gold.

REFERENCES

Akyüz, Y. (2021). External balance sheets of emerging economies: Low-yielding assets, high-yielding liabilities [Publisher: Edward Elgar Publishing Ltd]. *Review of Keynesian economics*, *9*(2), 232–252.

Ali, M. (2016). Global imbalances and asymmetric returns to US foreign assets: Fitting the missing pieces of the US balance of payments puzzle [Publisher: Routledge]. *International Review of Applied Economics*, *30*(2), 167–187. https://doi.org/10.1080/02692171.2015.1085002

Curcuru, S. E., Dvorak, T., & Warnock, F. E. (2008). Cross-border returns differentials [Publisher: MIT Press]. *The Quarterly Journal of Economics*, *123*(4), 1495–1530.

Curcuru, S. E., Dvorak, T., & Warnock, F. E. (2010). Decomposing the US external returns differential [Publisher: Elsevier]. *Journal of international Economics*, *80*(1), 22–32.

Curcuru, S. E., Thomas, C. P., & Warnock, F. E. (2013). On returns differentials [Publisher: Elsevier]. *Journal of International Money and Finance*, *36*, 1–25.

ERP. (2003). *Economic Report of the President* (tech. rep.). Executive Office of the President. Washington, D.C. https://www.presidency.ucsb.edu/sites/default/files/books/presidential-documents-archive-guidebook/the-economic-report-of-the-president-truman-1947-obama-2017/2003.pdf

Gilpin, R. (1971). The politics of transnational economic relations [Publisher: Cambridge University Press]. *International organization*, *25*(3), 398–419.

Godley, W. (2003). *The US economy: A changing strategic predicament*. Levy Economics Institute of Bard College Annandale-on-Hudson, NY. https://www.levyinstitute.org/pubs/stratpred.pdf

Gordon, R. (2017). *The rise and fall of American growth: The US standard of living since the civil war*. Princeton university press.

Gourinchas, P.-O., & Rey, H. (2007). From world banker to world venture capitalist: US external adjustment and the exorbitant privilege. In *G7 current account imbalances: Sustainability and adjustment* (pp. 11–66). University of Chicago Press.

Gourinchas, P.-O., & Rey, H. (2022). Exorbitant privilege and exorbitant duty [Publisher: CEPR Discussion Paper No. DP16944].

Gros, D. (2006). Why the US Current Account Deficit is Not Sustainable. *International Finance*, *9*(2).

Hausmann, R., & Sturzenegger, F. (2006). Global imbalances or bad accounting? The missing dark matter in the wealth of nations [Publisher: KSG Working Paper No. RWP06-003, Harvard CID Working Paper].

Hung, J. H., & Mascaro, A. (2004). *Return on Cross-Border Investment: Why Does U.S. Investment Abroad Do Better?* (Tech. rep. No. 16204). Congressional Budget Office. https://www.cbo.gov/sites/default/files/cbofiles/ftpdocs/60xx/doc6043/2004-17.pdf

Kindleberger, C. P. (1986). *The world in depression, 1929-1939*. Univ of California Press.

Mayer, J. (2021). The "exorbitant privilege" and "exorbitant duty" of the United States in the international monetary system: Implications for developing countries [Publisher: Springer]. *Review of World Economics*, *157*(4), 927–964.

Nievas, G., & Sodano, A. (2024). Has the US exorbitant privilege become a rich world privilege? Rates of return and foreign assets from a global perspective, 1970-2022.

Rogoff, K. (2025). *Our dollar, your problem: An insider's view of seven turbulent decades of global finance, and the road ahead*. Yale University Press.

Summers, L. H. (2016). US Economic Prospects: Secular Stagnation, Hysteresis, and the Zero Lower Bound [Publisher: Springer]. *The Best of Business Economics: Highlights from the First Fifty Years*, 421–435.

Summers, L. (2013). Presentation at the.

Waltz, K. (2018). *Man, the state, and war: A theoretical analysis*. Columbia University Press.

Williams, J. H. (1934). The world's monetary dilemma: Internal versus external monetary stability [Publisher: JSTOR]. *Proceedings of the Academy of Political Science*, *16*(1), 62–68.

Appendix

A Supplementary Descriptive Evidence

A.1 Positions: levels and shares of GDP

Figure A.1 documents the expansion of U.S. external positions since 2006. Direct-investment (DI) liabilities rise from roughly $3 trillion in 2006Q1 to about $16 trillion by 2025Q1, while DI assets increase from about $4 trillion to $11 trillion. Portfolio-investment (PI) liabilities grow even more, from roughly $8 trillion to $35 trillion, with PI assets moving from about $5 trillion to $16 trillion. The implied net positions (assets minus liabilities) therefore deteriorate over the period: DI moves from a small positive (about $1 trillion) to a sizable negative (around $5 trillion), and PI deepens from roughly $3 trillion to about $19 trillion.

Panel shares in Figure A.2 place these levels against the size of the U.S. economy. DI liabilities climb from roughly 20% of GDP in 2006 to about 75% by 2025, while DI assets rise from around 30% to about 50% of GDP; the DI net position swings from a modest surplus (about 7% of GDP) to a deficit near 25%. PI liabilities increase from roughly 50% of GDP to about 140%, with PI assets rising from around 30% to 70%. The PI net position widens from about -25% of GDP to roughly -70%.

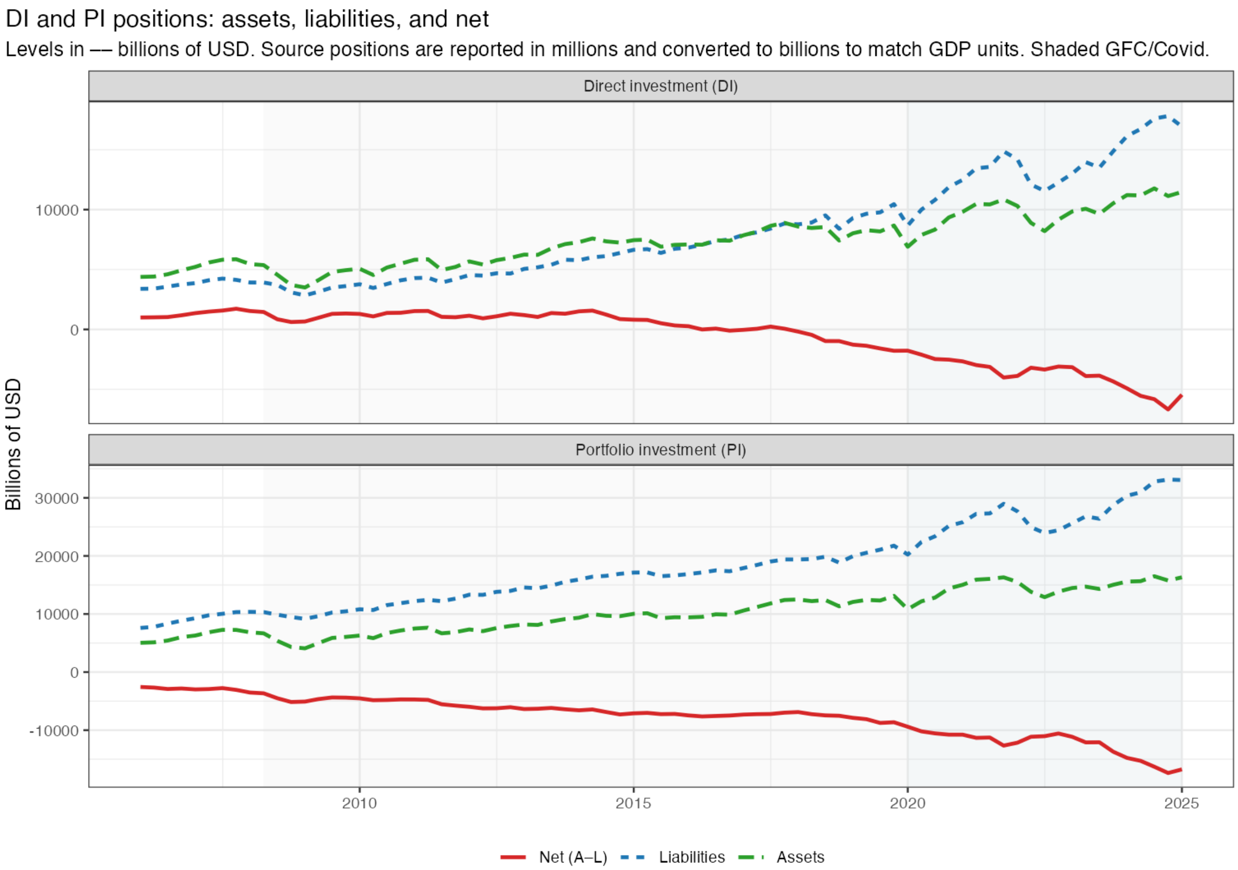

Figure A.1: Direct- and portfolio-investment positions (assets, liabilities, net) in billions of USD. Source positions are reported in millions and converted to billions; Net = Assets − Liabilities. Quarterly 2006Q1–2025Q1.

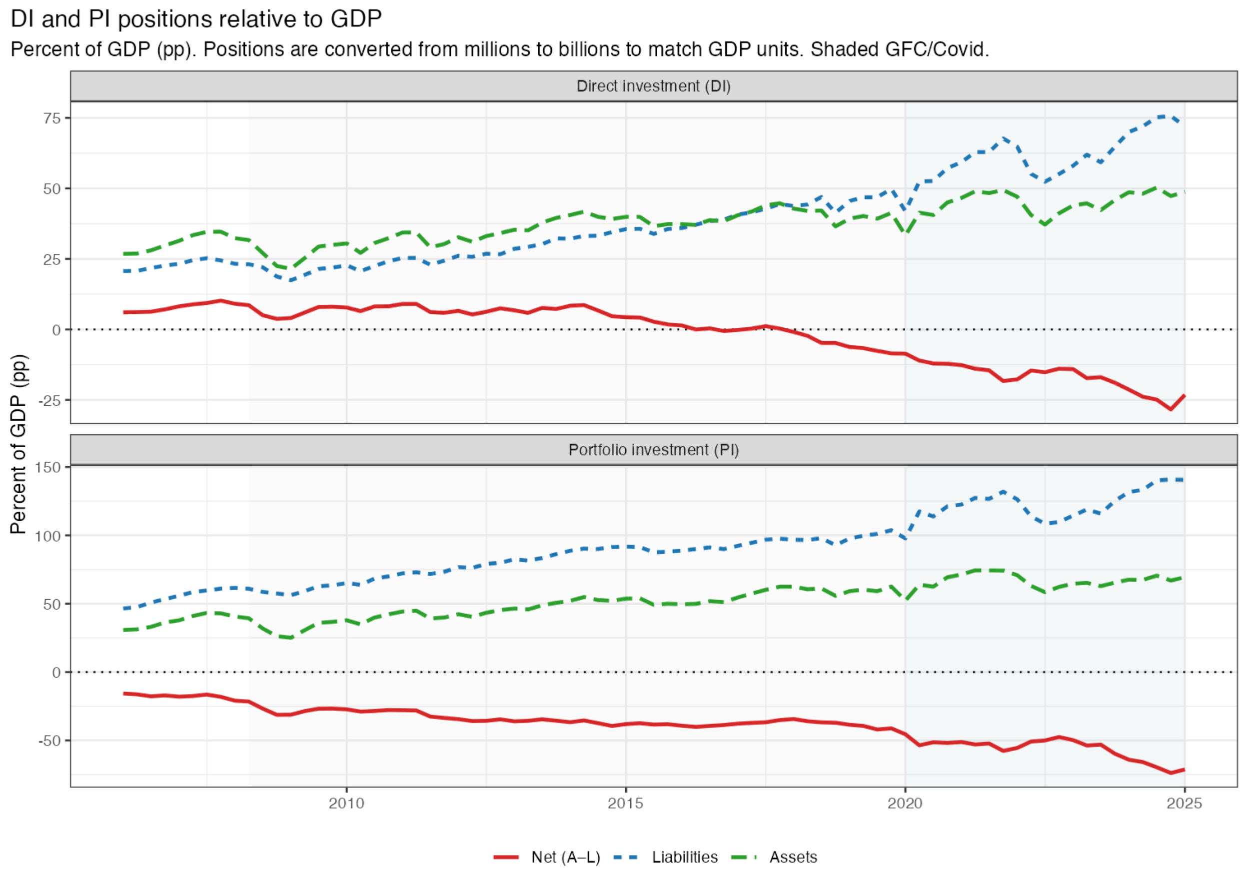

Figure A.2: Direct- and portfolio-investment positions as a share of GDP, in percentage points (pp) of GDP. Positions are converted from millions to billions, then scaled by GDP (billions). Quarterly 2006Q1–2025Q1.

Risk Composition

A.2 Risk vs. safe composition and overlays with DI/PI differentials

Risky vs. safe configuration (assets and liabilities). The United States is long risky assets (FDI and PI equity) and short safe liabilities (debt and bank/inter-office debt, plus reserves on the asset side). This "global insurer" configuration underlies the aggregate return effect.

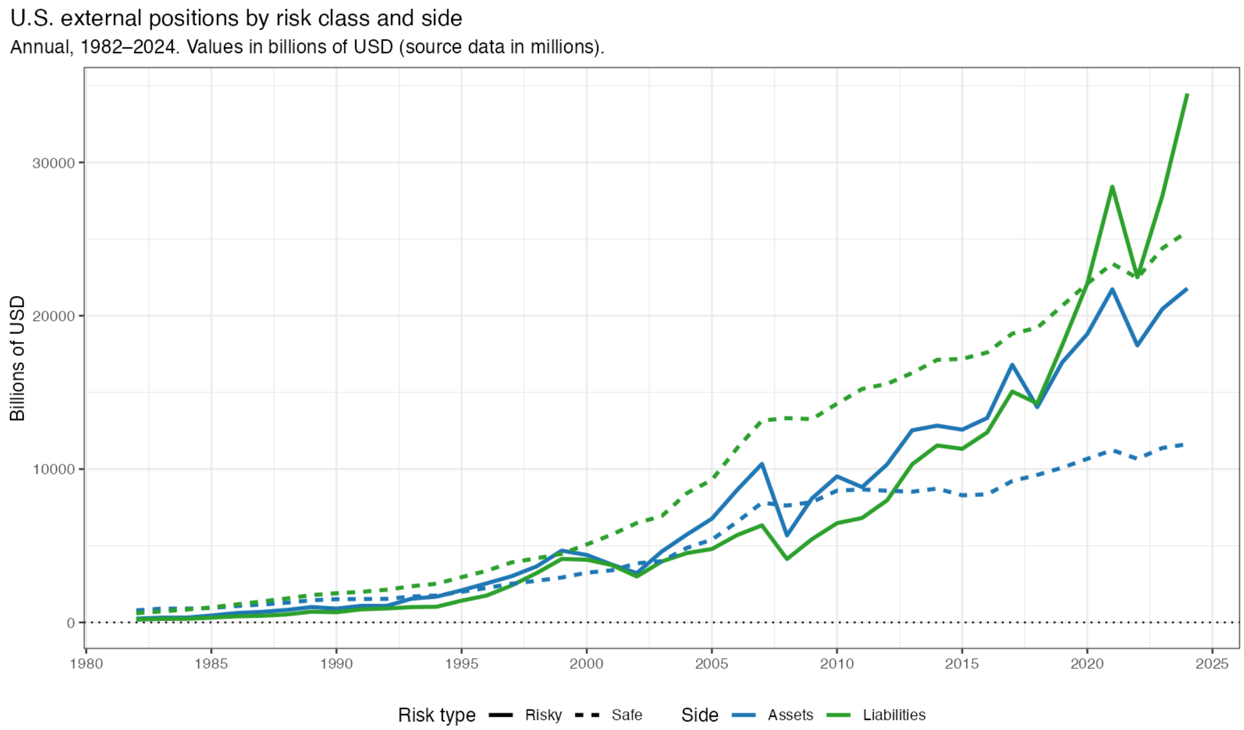

Figure A.3: U.S. external positions by risk class and side (assets vs. liabilities), annual 1982–2024. Values in billions of USD. Solid lines: risky; dashed: safe.

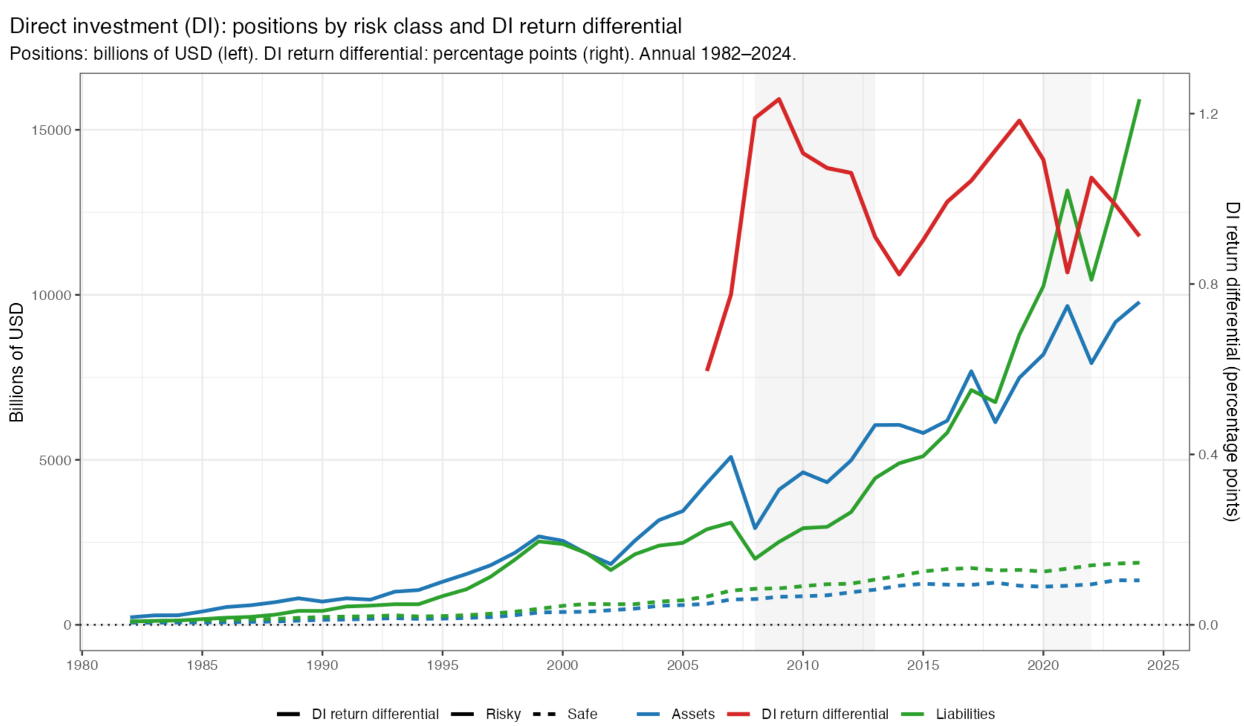

Figure A.4: Direct investment (DI): risky/safe assets and liabilities (left axis, billions of USD) and DI return differential (right axis, percentage points), annual 1982–2024. Shaded: 2008–2012 and 2020–2021.

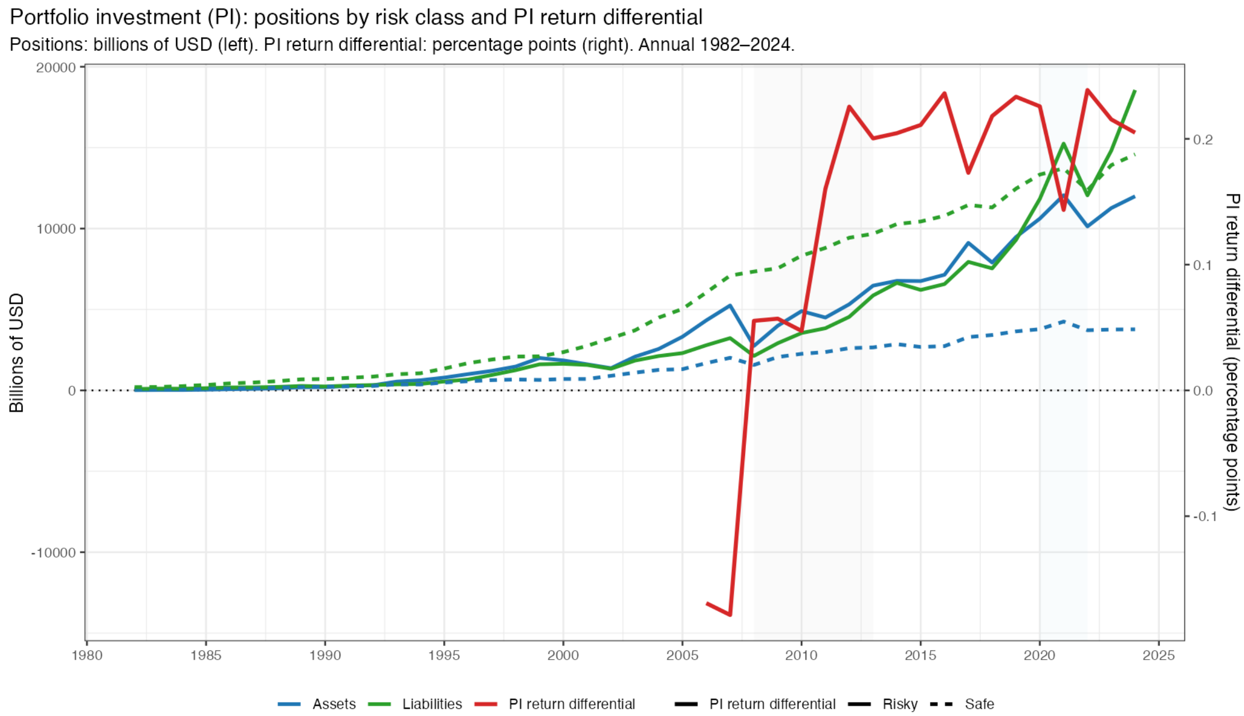

Figure A.5: Portfolio investment (PI): risky/safe assets and liabilities (left axis, billions of USD) and PI return differential (right axis, percentage points), annual 1982–2024. Shaded: 2008–2012 and 2020–2021.

A.3 Portfolio weights and return differential decomposition

Divergent stacked bars show that assets tilt toward risky categories (DI and PI equity) while liabilities tilt toward safe categories (PI debt and OI). This mix yields only a modest positive composition effect on average.

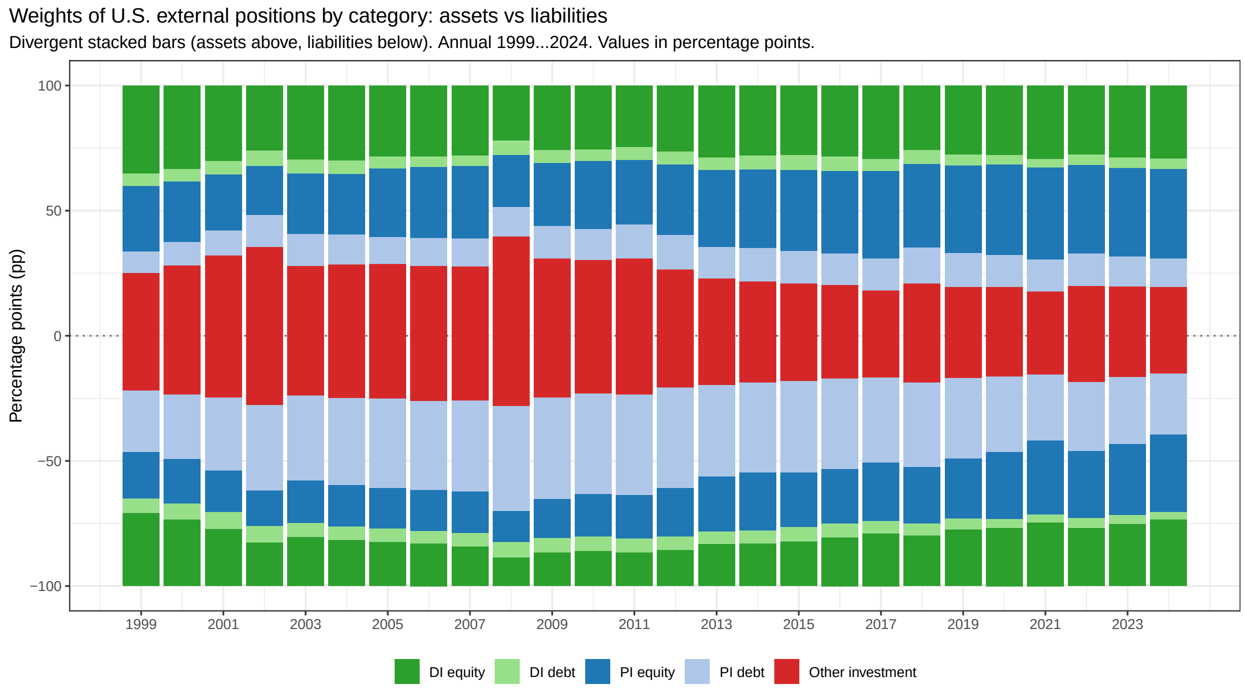

Figure A.6: Composition of U.S. external positions by category, with assets shown above zero and liabilities below. Divergent stacked bars, annual 1999–2024, expressed in percentage points. Notes: weights exclude financial derivatives other than reserves (IIP Table 1.1, assets line 5; liabilities line 13).

The decomposition clarifies that the U.S. external yield differential is driven mainly by return effects rather than by composition effects. Across all subperiods, the "Return" column in Table A.1 explains the bulk of the total differential, while the composition term is small and sometimes negative. Category-level rows show that direct investment (DI) equity is the workhorse: its return effect is large and positive in every subperiod, consistently contributing around one percentage point or more to the aggregate differential. In contrast, portfolio debt (PI debt) typically subtracts from the total—its "Total" entry is negative in most subperiods, reflecting either a liability-heavy composition, a low return gap, or both. DI debt and other investment are small in magnitude throughout.

The crisis chronology aligns with this pattern. During the GFC/Euro period, the aggregate differential remains positive because DI equity's return advantage offsets weakness elsewhere, whereas composition effects do little on net. In the post-crisis and Covid & after periods, the total differential edges higher largely on the back of DI equity returns, with modest support from PI equity; composition continues to play a limited role.

Table A.1: Yield differential decomposition by category and subperiod (pp).

2*Category	Pre-GFC (1999–2007)			GFC/Euro (2008–2012)			Post-crisis (2013–2019)			Covid & after (2020–2024)		
	Comp.	Return	Total	Comp.	Return	Total	Comp.	Return	Total	Comp.	Return	Total
Total	-0.2	1.3	1.1	-0.0	1.4	1.5	0.1	1.9	1.9	0.0	1.9	1.6
DI equity	0.5	1.1	1.6	0.8	1.5	2.3	0.4	1.2	1.5	0.2	1.2	1.3
DI debt	-0.0	-0.1	-0.1	-0.0	-0.2	-0.2	0.0	-0.1	-0.0	0.0	-0.0	-0.0
PI equity	0.2	0.1	0.3	0.2	0.6	0.8	0.2	0.7	0.9	0.2	0.4	0.5
PI debt	-1.1	0.1	-1.0	-1.1	-0.5	-1.6	-0.6	0.0	-0.6	-0.4	0.2	-0.3
Other investment	0.2	0.1	0.3	0.0	-0.1	-0.1	0.1	0.0	0.1	0.1	0.1	0.1

Notes: Values are subperiod means of annual percentage-point contributions. “Comp.” is the composition effect; “Return” is the within-category return-gap effect; “Total” equals the sum of the two (up to rounding). Subperiod order is Pre-GFC, GFC/Euro, Post-crisis, and Covid & after.

B Diagnostics

Table B.1: Lag-length selection for the VARX(p) with exogenous controls (VIX, GFC, Covid)

Criterion	**Selected lag $\hat{p}$**
AIC	8
HQ	8
SC (BIC)	1
FPE	8

Notes: Search range $p \in \{1, \dots, 8\}$. Endogenous block: (CAGDP, g^*, g, REER, FFR, r_{diff}). Exogenous: (VIX, GFC, Covid). AIC/HQ/FPE favor a rich lag structure; SC/BIC favors parsimony. Baseline in the paper sets $p = 2$ and validates adequacy by stability and LM tests.

Table B.2: Consolidated unit-root evidence (ADF, PP, KPSS), 2006Q1–2025Q1

	ADF (ur.df)				PP (Z_τ)				KPSS				
Variable	L(d)	L(t)	Δ(d)	Δ(t)	L(d)	L(t)	Δ(d)	Δ(t)	L(μ)	L(τ)	Δ(μ)	Δ(τ)	Verdict
CAGDP	NR	NR	R	R	NR	NR	R	R	R	R	R	NR	I(1) (minor KPSS-$\Delta\mu$ inconsistency)
g	R	NR	R	R	NR	NR	R	R	NR	NR	NR	NR	I(0) / borderline
g^*	R	R	R	R	R	R	R	R	NR	NR	NR	NR	I(0)
REER	NR	NR	R	R	NR	NR	R	R	R	R	NR	NR	I(1)
FFR	NR	NR	R	NR	NR	NR	R	R	NR	R	NR	NR	I(1)
r_diff	NR	NR	R	R	NR	NR	R	R	R	R	NR	NR	I(1)

Notes. Entries show decisions at the 5% level: **ADF** and **PP** test H_0: unit root (R = reject unit root; NR = fail to reject); **KPSS** tests H_0: (level/trend) stationarity (R = reject stationarity; NR = fail to reject). "d/t" denote drift (constant) / trend (constant+trend) deterministic components; "L" = levels, "Δ" = first differences. ADF decisions are based on the τ statistic under each deterministic spec (drift or trend) using 5% critical values; a 10% rejection does not count as R here. Verdict synthesizes across tests with priority on agreement between ADF/PP in levels vs. differences and the KPSS direction of evidence. The small KPSS inconsistency for CAGDP in first differences does not overturn the I(1) classification given strong ADF/PP rejections in Δ.

Table B.3: Consolidated unit-root evidence (ADF, PP, KPSS), 2006Q1–2025Q1

	ADF (ur.df)				PP (Z_τ)				KPSS				
Variable	L(d)	L(t)	Δ(d)	Δ(t)	L(d)	L(t)	Δ(d)	Δ(t)	L(μ)	L(τ)	Δ(μ)	Δ(τ)	Verdict
CAGDP	NR	NR	R	R	NR	NR	R	R	R	R	R	NR	I(1) (minor KPSS-$\Delta\mu$ inconsistency)
g	R	NR	R	R	NR	NR	R	R	NR	NR	NR	NR	I(0) / borderline
g^*	R	R	R	R	R	R	R	R	NR	NR	NR	NR	I(0)
REER	NR	NR	R	R	NR	NR	R	R	R	R	NR	NR	I(1)
FFR	NR	NR	R	NR	NR	NR	R	R	NR	R	NR	NR	I(1)
r_diff	NR	NR	R	R	NR	NR	R	R	R	R	NR	NR	I(1)

Notes. Entries show decisions at the 5% level: **ADF** and **PP** test H_0: unit root (R = reject unit root; NR = fail to reject); **KPSS** tests H_0: (level/trend) stationarity (R = reject stationarity; NR = fail to reject). “d/t” denote drift (constant) / trend (constant+trend) deterministic components; “L” = levels, “Δ” = first differences. ADF decisions are based on the τ statistic under each deterministic spec (drift or trend) using 5% critical values; a 10% rejection does not count as R here. Verdict synthesizes across tests with priority on agreement between ADF/PP in levels vs. differences and the KPSS direction of evidence. The small KPSS inconsistency for CAGDP in first differences does not overturn the I(1) classification given strong ADF/PP rejections in Δ.

Table B.7: System-wide ARCH-LM tests for heteroskedasticity (VARX p=2, total spec).

Test	**Lag order**
ARCH-LM (system-wide)	1, 2, 4, 8, 12

Table B.8: Per-equation ARCH-LM tests for heteroskedasticity (VARX p=2, total spec).

Equation	**Lag**	**Statistic**	**p-value**	**Decision (5%)**
r_diff_pp	1	2.46	0.117	Fail to reject
	2	5.29	0.071	Borderline (10%)
	4	6.02	0.198	Fail to reject
	8	8.24	0.410	Fail to reject
	12	14.17	0.290	Fail to reject
g_star	1	3.83	0.050	Borderline
	2	3.78	0.151	Fail to reject
	4	12.16	0.016	Reject
	8	14.71	0.065	Borderline (10%)
	12	14.03	0.299	Fail to reject
g	1	6.07	0.014	Reject
	2	8.02	0.018	Reject
	4	14.09	0.007	Reject
	8	18.47	0.018	Reject
	12	18.18	0.111	Fail to reject
FFR	1	2.66	0.103	Fail to reject
	2	3.05	0.217	Fail to reject
	4	3.72	0.445	Fail to reject
	8	4.59	0.800	Fail to reject
	12	10.52	0.573	Fail to reject
REER	1	0.13	0.717	Fail to reject
	2	1.15	0.562	Fail to reject
	4	4.78	0.311	Fail to reject
	8	7.51	0.483	Fail to reject
	12	8.72	0.726	Fail to reject
CAGDP	1	0.03	0.855	Fail to reject
	2	0.19	0.908	Fail to reject
	4	2.92	0.571	Fail to reject
	8	18.53	0.018	Reject
	12	37.27	0.000	Reject

Table B.4: VAR stability diagnostics: roots of the characteristic polynomial

Model (tag)	Endog. vars.	Lags p	# Roots	$\max\|\lambda\|$	Any $\|\lambda\| \geq 1$?	Verdict
`total_varx_p1_base`	6	1	6	0.9836		Stable
`total_varx_p2_base`	6	2	12	0.9513		Stable

Notes: Stability requires all eigenvalues of the VAR companion matrix to lie strictly inside the unit circle. Entries report the number of roots, the largest modulus $\max|\lambda|$, and whether any modulus is ≥ 1. Values are computed from the saved models' root spectra; both specifications satisfy the stability condition.

Table B.5: Residual autocorrelation diagnostics for the baseline VARX(p=2), sample 2006Q1–2025Q1

Panel A. Breusch–Godfrey LM per equation: p-values at lag h

Equation	h=4	h=8	h=12
CAGDP	0.508	0.633	0.801
g	0.001***	0.001***	0.000***
g^*	0.000***	0.003***	0.008***
REER	0.421	0.492	0.535
FFR	0.908	0.885	0.739
r_{diff} (pp)	0.505	0.787	0.561

Panel B. System–wide tests (statistic, df, p-value)

Test	h	Stat	p-value
Breusch–Godfrey LM	4	237.629 (df=144)	0.000***
Breusch–Godfrey LM	8	393.023 (df=288)	0.000***
Breusch–Godfrey LM	12	450.000 (df=432)	0.265
Portmanteau (adjusted)	4	125.488 (df=72)	0.000***
Portmanteau (adjusted)	8	252.434 (df=216)	0.045**
Portmanteau (adjusted)	12	391.362 (df=360)	0.123
Portmanteau (asympt.)	4	120.517 (df=72)	0.000***
Portmanteau (asympt.)	8	237.021 (df=216)	0.156
Portmanteau (asympt.)	12	356.516 (df=360)	0.542

Notes: Stars mark significance at 10% (*), 5% (**), 1% (***). Panel A reports equation-by-equation Breusch–Godfrey LM p-values for the null of no residual autocorrelation at lags $h \in \{4, 8, 12\}$. Panel B reports system-wide Breusch–Godfrey LM and Portmanteau tests. Portmanteau (asympt.) at h=12 fails to reject serial independence (p=0.542).[a]

Table B.6: Residual normality tests for VARX(2), total specification

Equation	JB statistic	p-value	Normality decision (5%)
r^{diff} (total return differential, pp)	2.56	0.28	Fail to reject normality
g^* (foreign GDP growth)	455.03	0.000	Reject normality
g (US GDP growth)	29.23	0.000	Reject normality
FFR (US Fed funds rate)	0.93	0.63	Fail to reject normality
REER (real effective exchange rate)	1.00	0.61	Fail to reject normality
CAGDP (current account / GDP)	25.92	0.000	Reject normality
Multivariate tests (system-wide)			
Joint Jarque–Bera	537.5	0.000	Reject normality
Skewness component	50.4	0.000	Reject normality
Kurtosis component	487.0	0.000	Reject normality

Notes: JB = Jarque–Bera test for residual normality. The null hypothesis is that residuals are i.i.d. Gaussian. “Fail to reject” means residuals are not significantly different from Gaussian at the 5% level.

C GENERALIZED (REDUCED-FORM) VARX IRFS

(a) CA/GDP to RD shock (+1 pp)

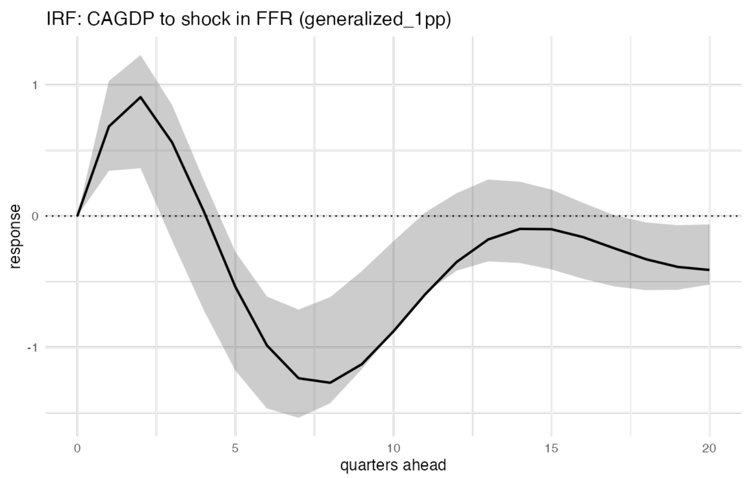

(b) CA/GDP to FFR shock (1 s.d.)

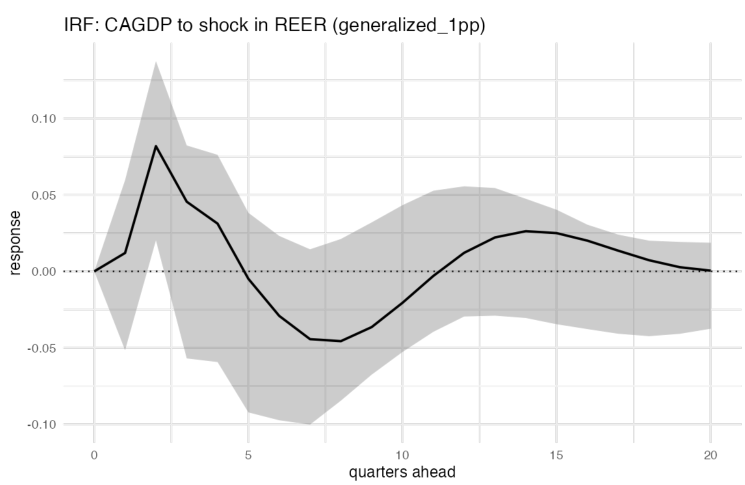

(c) CA/GDP to REER shock (1 s.d.)

Figure C.1: Generalized IRFs for the current account. Lines show median responses; shaded areas are bootstrap bands (68%). The return-differential shock is scaled to a +1 percentage-point move in r_{diff} on impact; other shocks are one–standard-deviation innovations. Horizons in quarters.

Table B.9: Structural stability diagnostics: coefficient tests and variance breaks (VARX, $p = 2$, total specification).

	Coefficient stability tests			Variance breaks (Bai–Perron)	
Equation	supF (p)	aveF (p)	expF (p)	# Breaks	Break dates
r_diff^{pp}	32.6 (0.102)	24.9 (0.0267)	13.9 (0.0672)	0	—
g^*	801.0 (0.000)	140.0 (0.000)	397.0 (0.000)	2	2019Q3; 2022Q2
g	105.0 (1.29×10^{-13})	48.5 (1.12×10^{-7})	—	0	—
FFR	—	—	—	0	—
REER	—	—	—	0	—
CAGDP	—	—	—	1	2021Q4

Table B.10: Granger causality tests of return differentials on the U.S. current account balance (2006Q1–2025Q1).

Specification	**Cause variables**	**Target**	**Test statistic**	**df**	**p-value**
Simple Granger (Wald)	r_diff_pp	CAGDP	3.88	10	0.00005
Block exogeneity (manual Wald)	r_diff_pp, REER, FFR	CAGDP	27.20	6	0.00013
Toda–Yamamoto robust VAR	r_diff_pp	CAGDP	19.03	2	0.00007

Notes: The table reports Wald test statistics for the null hypothesis that the lagged values of the "cause" variables do not Granger-cause the U.S. current account balance to GDP (CAGDP). The block exogeneity test jointly restricts lag coefficients of return differentials, the real effective exchange rate (REER), and the federal funds rate (FFR). The Toda–Yamamoto test augments the VAR with $p + d_{\max}$ lags (here $p = 2$, $d_{\max} = 1$) to ensure validity under potential unit roots. All specifications include VIX, GFC, and Covid as exogenous controls.

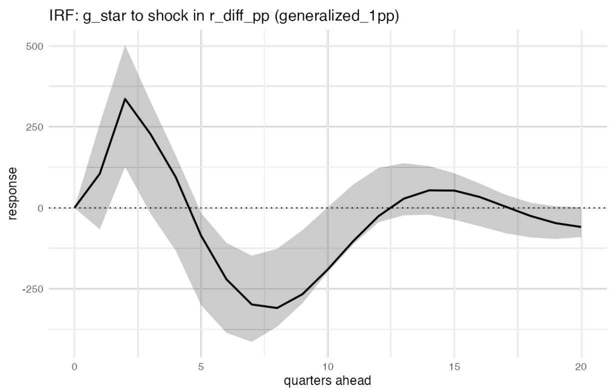

(a) $g^* \to r_{\text{diff}}$

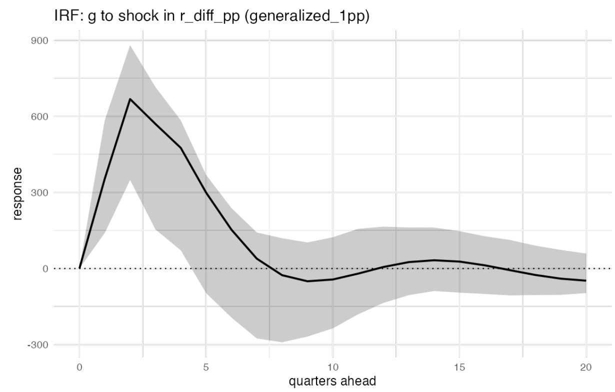

(b) $g \to r_{\text{diff}}$

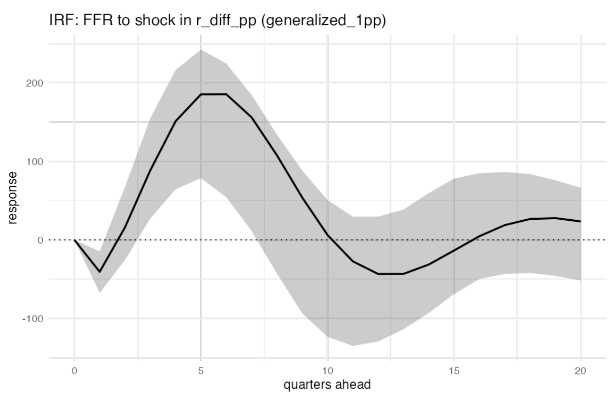

(c) FFR $\to r_{\text{diff}}$

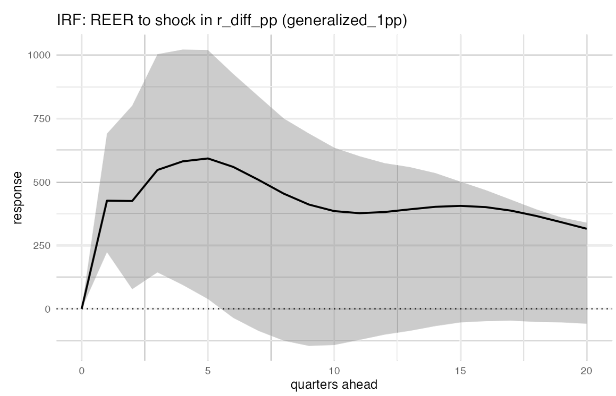

(d) REER $\to r_{\text{diff}}$

Figure C.2: Generalized IRFs for the return differential. Responses are in percentage points of r_{diff}. Shocks to g, g^*, FFR, REER are one–standard-deviation innovations; bands are bootstrap 68%.

D Joint SR–SVAR impulse responses and robustness

Impulse responses. Figure 6.1 shows the 2x2 panel of CA/GDP responses to DI, PI, MP, and REER shocks (median with 90% bands). DI shocks consistently reduce CA/GDP, while PI shocks are smaller and more ambiguous. MP and REER shocks also push CA/GDP lower, but with modest magnitudes.

Posterior sign shares. Because sign-restricted identification averages over many admissible rotations, uncertainty bands often touch zero. Robustness is therefore summarized in Figure D.1, which reports posterior sign shares (the fraction of admissible models with $\Delta CA/GDP < 0$). DI shocks exhibit robust directionality (~60–80% probability of negative responses across horizons), while PI shocks are closer to indeterminate (below 50% near term, rising toward 50–55% at longer horizons). MP shocks hover around 40–50%, whereas REER shocks exceed 50% in the medium run.

Direction-aware robustness. Figure D.2 contrasts DI and PI shocks directly. Under the baseline identification (Stage 2), DI shocks reduce CA/GDP with high probability ($P[\text{IRF} \leq 0] \approx 0.8$–$0.9$), whereas PI shocks remain weakly identified, with posterior mass around zero. To probe robustness, I impose a weak inequality prior (PI ≥ 0 on impact), trimming implausible negative draws without altering the overall IRF profile. Conditional on this prior, the probability that PI shocks increase CA/GDP rises to ~0.7–0.8 at short horizons. This should be read not as a new baseline but as a sensitivity check highlighting the fragility of PI identification.

Alternative PI variants. Figure D.3 compares the baseline PI response with two weak-prior variants (impact ≥ 0 and cumulative ≥ 0 over four quarters). All three profiles remain close to zero in the short run, drifting slightly negative or positive depending on the prior. The exercise reinforces that PI shocks do not deliver strong or robust effects on CA/GDP, unlike DI shocks.

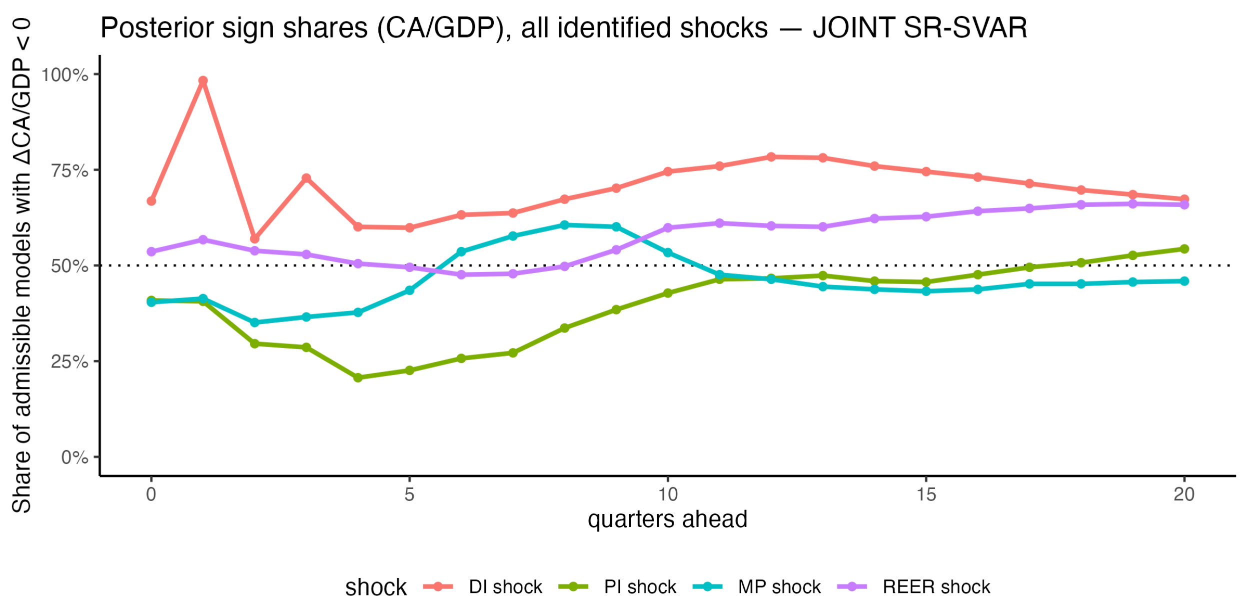

Figure D.1: Posterior sign shares for CA/GDP (share of admissible rotations with $\Delta CA/GDP < 0$) for DI, PI, MP, and REER shocks.

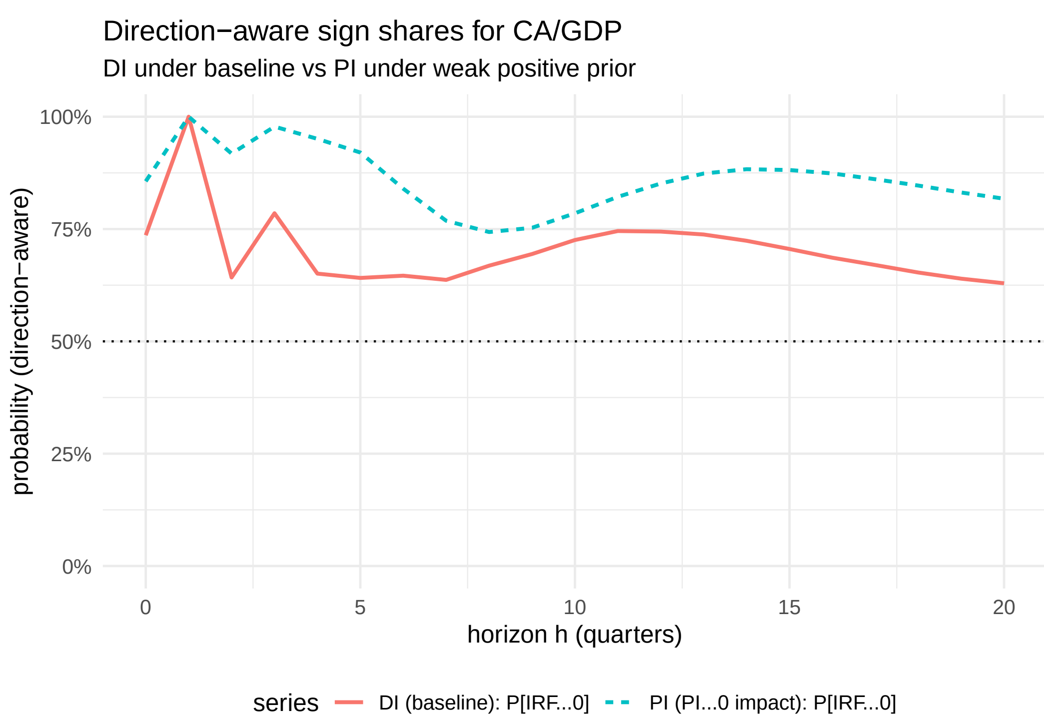

Figure D.2: Direction-aware sign shares for CA/GDP responses. The red line shows the unconditional baseline probability that DI shocks reduce CA/GDP ($P[\text{IRF} \leq 0]$). The blue line shows the conditional probability that PI shocks increase CA/GDP under the weak inequality prior ($P[\text{IRF} \geq 0]$). Both are well above 0.5, but only the DI case provides unconditional directionality; the PI case is conditional and should be interpreted as suggestive evidence.

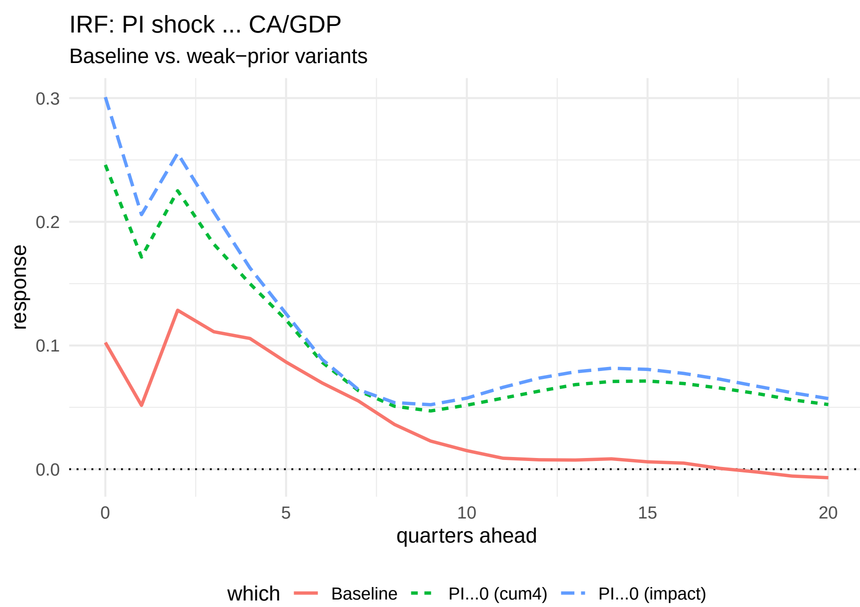

Figure D.3: Impulse responses of CA/GDP to a portfolio return-differential (PI) shock under the baseline sign set and two weak-prior variants (PI≥ 0 on impact and PI≥ 0 cumulatively over four quarters).

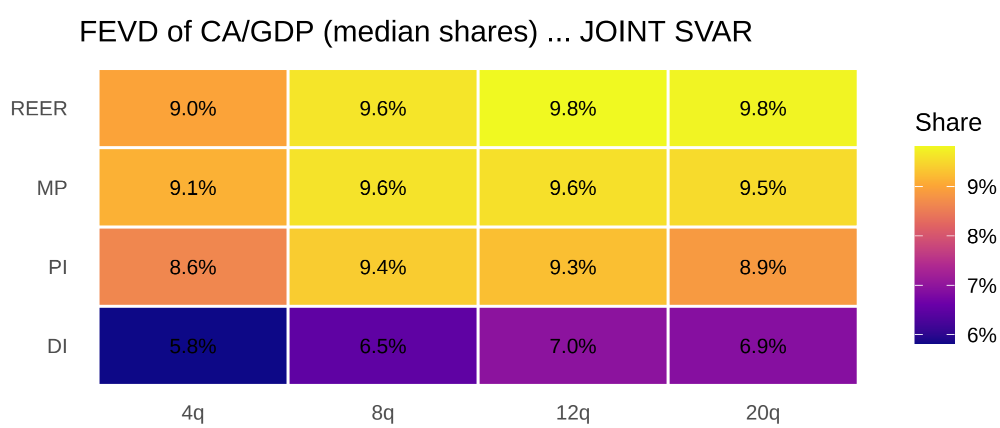

Figure D.4: Heatmap of median FEVD shares of CA/GDP in the Joint SR–SVAR. Darker cells indicate larger contributions. Shares need not sum to 100%.

Additional FEVD evidence

Heatmap. Figure D.4 presents a heatmap of FEVD medians by horizon, a compact way of showing the same information as Table 6.1. Darker cells indicate larger contributions, and labels report percentages.

Unified FEVD table with PI restrictions. Table D.1 reports FEVD shares under the baseline identification and under weak PI≥ 0 restrictions (impact or cumulative over four quarters). PI shares increase modestly under the restrictions, but the qualitative ranking is unchanged: PI explains more of the variance than DI, regardless of the prior.

Table D.1: FEVD of CA/GDP under baseline and PI sign restrictions

Horizon	Shock	Baseline	PI≥0 (h1)	PI≥0 (cum4)
4	DI	0.058	0.078	0.085
	PI	0.086	0.130	0.100
	MP	0.091	0.078	0.086
	REER	0.090	0.083	0.087
8	DI	0.065	0.086	0.090
	PI	0.094	0.135	0.107
	MP	0.096	0.084	0.091
	REER	0.096	0.089	0.094
12	DI	0.070	0.088	0.092
	PI	0.093	0.135	0.109
	MP	0.096	0.087	0.093
	REER	0.098	0.092	0.095
20	DI	0.069	0.086	0.092
	PI	0.089	0.136	0.109
	MP	0.095	0.086	0.092
	REER	0.098	0.090	0.093